

# Prospects for charged Higgs bosons in natural SUSY models at the high-luminosity LHC

Howard Baer<sup>1,2\*</sup>, Vernon Barger<sup>2†</sup>, Xerxes Tata<sup>3‡</sup> and Kairui Zhang<sup>2‡</sup>

<sup>1</sup>*Homer L. Dodge Department of Physics and Astronomy, University of Oklahoma, Norman, OK 73019, USA*

<sup>2</sup>*Department of Physics, University of Wisconsin, Madison, WI 53706 USA*

<sup>3</sup>*Department of Physics and Astronomy, University of Hawaii, Honolulu, HI 53706 USA*

## Abstract

We continue our examination of prospects for discovery of heavy Higgs bosons of natural SUSY (natSUSY) models at the high luminosity LHC (HL-LHC), this time focussing on charged Higgs bosons. In natSUSY, higgsinos are expected at the few hundred GeV scale whilst electroweak gauginos inhabit the TeV scale and the heavy Higgs bosons,  $H$ ,  $A$  and  $H^\pm$  could range up tens of TeV without jeopardizing naturalness. For TeV-scale heavy SUSY Higgs bosons  $H$ ,  $A$  and  $H^\pm$ , as currently required by LHC searches, SUSY decays into gaugino plus higgsino can dominate  $H^\pm$  decays provided these decays are kinematically accessible. The visible decay products of higgsinos are soft making them largely invisible, whilst the gauginos decay to  $W$ ,  $Z$  or  $h$  plus missing transverse energy ( $\cancel{E}_T$ ). Charged Higgs bosons are dominantly produced at LHC14 via the parton subprocess,  $gb \rightarrow H^\pm t$ . In this paper, we examine the viability of observing signatures from  $H^\pm \rightarrow \tau\nu$ ,  $H^\pm \rightarrow tb$  and  $H^\pm \rightarrow W, Z, h + \cancel{E}_T$  events produced in association with a top quark at the HL-LHC over large Standard Model (SM) backgrounds from (mainly)  $t\bar{t}$ ,  $t\bar{t}V$  and  $t\bar{t}h$  production (where  $V = W, Z$ ). We find that the greatest reach is found via the SM  $H^\pm(\rightarrow \tau\nu) + t$  channel with a subdominant contribution from the  $H^\pm(\rightarrow tb) + t$  channel. Unlike for neutral Higgs searches, the SUSY decay modes appear to be unimportant for  $H^\pm$  searches at the HL-LHC. We delineate regions of the  $m_A$  vs.  $\tan\beta$  plane, mostly around  $m_A \sim 1 - 2$  TeV, where signals from charged Higgs bosons would serve to confirm signals of a heavy, neutral Higgs boson at the  $5\sigma$  level or, alternatively, to exclude heavy Higgs bosons at the 95% confidence level at the high luminosity LHC.

---

\*Email: baer@ou.edu

†Email: barger@pheno.wisc.edu

‡Email: tata@phys.hawaii.edu

‡Email: kzhang89@wisc.edu

# 1 Introduction

There are two routes to discovery of supersymmetry (SUSY) at hadron colliders such as the CERN Large Hadron Collider (LHC): one is via direct pair production of  $R$ -parity odd states and the other is via single (or pair) production of new  $R$ -parity even states such as the additional heavy Higgs bosons present in the Minimal Supersymmetric Standard Model (MSSM) [1]. Of course, strictly speaking, the production of the heavy Higgs boson states is not necessarily a signal for supersymmetry (unless these are seen via their decays into supersymmetric particles) since such states are also possible in non-supersymmetric models with an extended Higgs sector. In the present paper, we continue our work on the second approach: prospects for SUSY discovery via the required additional SUSY Higgs bosons. While much work has been done in this field, our focus is on LHC signals of the heavy Higgs bosons of *natural* SUSY models, wherein no large fine-tunings are required in order to gain a weak scale characterized by  $m_{W,Z,h} \simeq 100$  GeV. In previous work, we examined prospects for SUSY Higgs discovery in natural SUSY via resonance production of heavy neutral Higgs bosons  $H$  and  $A$ , followed by 1. decays into Standard Models modes with  $H, A \rightarrow \tau^+\tau^-$  being most promising [2], and 2. decays into pairs of SUSY particles [3] which offer qualitatively new channels for SUSY Higgs boson discovery. Within natural SUSY, once the heavy Higgs boson decay channels to gaugino+higgsino become open, these may rapidly dominate the branching fractions. This leads to two effects: 1. the new SUSY decay modes diminish the branching fractions into SM modes, thus diminishing the expected LHC reach via these decay channels, and 2. the new SUSY decay modes open up new avenues for SUSY Higgs detection, where these new channels would signal the presence of the expected SUSY particles. In the present paper, we extend our earlier analyses to include production of charged SUSY Higgs bosons  $H^\pm$ . Discovery of charged SUSY Higgs bosons is expected to be more challenging than discovery of the neutral bosons. This is due to typically smaller production cross sections (for a given Higgs boson mass) but also to less distinctive discovery signatures. We investigate here whether this situation still maintains under the rubric of natural SUSY.

Here, we take the measured value of the  $Z$ -boson mass as representative of the magnitude of weak scale, where in the MSSM the  $Z$  mass is related to the weak scale Lagrangian parameters via the electroweak minimization condition

$$m_Z^2/2 = \frac{m_{H_d}^2 + \Sigma_d^d - (m_{H_u}^2 + \Sigma_u^u) \tan^2 \beta}{\tan^2 \beta - 1} - \mu^2 \quad (1)$$

where  $m_{H_u}^2$  and  $m_{H_d}^2$  are the Higgs soft breaking masses,  $\mu$  is the (SUSY preserving) superpotential higgsino mass parameter and the  $\Sigma_d^d$  and  $\Sigma_u^u$  terms contain a large assortment of loop corrections (see Appendices of Ref. [4] and [5] and also [6] for leading two-loop corrections). We adopt the notion of *practical naturalness* [7, 8], wherein the value of an observable  $\mathcal{O}$  is natural if all *independent* contributions to  $\mathcal{O}$  are comparable to (within a factor of few), or smaller than  $\mathcal{O}$ . For natural SUSY models, we use the naturalness measure [4, 9]

$$\Delta_{EW} \equiv |\text{maximal term on the right-hand-side of Eq. (1)}|/(m_Z^2/2), \quad (2)$$

and take

$$\Delta_{EW} \lesssim 30 \quad (3)$$

to be natural. For most SUSY benchmark models, the superpotential  $\mu$  parameter is tuned to cancel against large contributions to the weak scale from SUSY breaking. Since the  $\mu$  parameter typically arises from very different physics than SUSY breaking, *e.g.* from whatever solution to the SUSY  $\mu$  problem that is assumed,<sup>1</sup> then such a “just-so” cancellation is highly implausible [11] (though logically possible) compared to the case where all contributions to the weak scale are  $\sim m_{weak}$ , so that  $\mu$  (or other parameters) need not be tuned.

Several important implications of Eq. (3) for heavy SUSY Higgs searches include the following.

- The superpotential  $\mu$  parameter enters  $\Delta_{EW}$  directly, leading to  $|\mu| \lesssim 350$  GeV. This implies that for heavy Higgs searches with  $m_{H^\pm} \gtrsim 2|\mu|$ , then SUSY decay modes of  $H^\pm$  should typically be open. If these additional decay widths to SUSY particles are large, then the branching fractions to the (usually assumed) SM search modes would be correspondingly reduced.
- For  $|m_{H_d}^2| \gg |m_{H_u}^2|$  or  $\mu^2$ , then  $|m_{H_d}|$  sets the heavy Higgs mass scale ( $m_{A,H,H^\pm} \sim |m_{H_d}|$ ) while  $|m_{H_u}|$  sets the mass scale for  $m_{W,Z,h}$ . Then, assuming that  $m_{H^\pm} \gg M_W$ , naturalness requires [12]

$$m_{A,H,H^\pm} \lesssim m_Z \tan \beta \sqrt{\Delta_{EW}}. \quad (4)$$

For  $\tan \beta \sim 10$  with  $\Delta_{EW} \lesssim 30$ , then  $m_{H^\pm}$  can range up to  $\sim 5$  TeV. For  $\tan \beta \sim 40$ , then  $m_{H^\pm}$  stays natural up to  $\sim 20$  TeV (although for large  $\tan \beta \gtrsim 20$ , then bottom squark contributions to  $\Sigma_u^u$  become large and provide much stronger upper limits on natural SUSY spectra [7]).

In Sec. 2, we first present a natural SUSY benchmark point which then leads to a natural SUSY Higgs scenario which we previously dubbed  $m_H^{125}(\text{nat})$ . The  $m_h^{125}(\text{nat})$  scenario is promoted as a template for SUSY Higgs searches in that [2] 1. it leads to a value of  $m_h \simeq 125$  GeV throughout almost the entire  $m_A$  vs.  $\tan \beta$  search plane and 2. the value of  $\Delta_{EW}$  is also low (though sometimes exceeding a value of 30 at higher  $\tan \beta$  values) throughout the search plane. In Sec. 3, we list the dominant charged SUSY Higgs boson production cross sections at LHC14 (LHC with  $\sqrt{s} = 14$  TeV). It is well-known that the  $gb \rightarrow tH^\pm$  subprocesses is the dominant  $H^\pm$  production mechanism at the LHC [13–15]. In Sec. 4, we present charged Higgs boson branching fractions from the  $m_h^{125}(\text{nat})$  scenario in the  $m_A$  vs.  $\tan \beta$  plane, and find that indeed SUSY decay modes do become rapidly dominant once these are kinematic accessible. In Sec. 5, we examine  $pp \rightarrow tH^\pm + X$  followed by  $H^\pm \rightarrow \tau^\pm \nu_\tau$  and map out distributions which help obtain signal over SM background levels. In Sec. 6, we examine  $pp \rightarrow tH^\pm + X$  followed by  $H^\pm \rightarrow tb$  decay. In Sec. 7, we study the impact of the SUSY decays of  $H^\pm$  bosons: unfortunately, we find that the relevant cross-sections are mostly in the sub-fb range for mass values where the branching fractions for these modes become substantial, and (contrary to what we found for  $H$  and  $A$  bosons) SUSY decays of  $H^\pm$  do not offer a viable search strategy. In Sec. 8, we plot out the reach of high-luminosity LHC for charged Higgs bosons of natural SUSY. Our summary and conclusions are contained in Sec. 9.

---

<sup>1</sup>Twenty solutions to the SUSY  $\mu$  problem are recently reviewed in Ref. [10].

## 1.1 A review of some previous related work

Here, we present a brief (and likely incomplete) review of some related work on charged Higgs bosons from SUSY. In Ref. [16], it was already emphasized that detection of a top quark signal in accord with SM expectations would preclude the decay  $t \rightarrow bH^+$  and thus require  $m_{H^\pm} \gtrsim m_t - m_b$ . In light of present  $t\bar{t}$  signal results, this implies  $m_{H^\pm} \gtrsim 168$  GeV. This result was already used by Kunszt and Zwirner in Ref. [17] to form the low  $m_A$  limit of the proposed  $m_A$  vs.  $\tan\beta$  heavy SUSY Higgs search plane. Decays of heavy SUSY Higgs boson to SUSY decay modes were originally explored in Ref. [18–21] and the complete set of  $H^\pm$  decay widths may be found in Appendix C of [1]. In Ref. [12], these decay modes were examined in the context of natural SUSY. In that work, it was noted that for  $H$ ,  $A$ ,  $H^\pm \rightarrow \text{wino} + \text{higgsino}$  channels, the higgsino decays led to mainly soft, quasi-visible decay debris whilst the winos decayed dominantly via two-body modes into  $W + \text{higgsino}$ ,  $Z + \text{higgsino}$  and  $h + \text{higgsinos}$ .

In Ref. [13–15], it was found that the dominant production process for charged Higgs bosons at LHC was the reaction  $gb \rightarrow tH^- + \text{c.c.}$ . NLO corrections to this production process were calculated in Ref. [22, 23] and [24]. Signals from the final state  $tH^\pm (\rightarrow \tau\nu_\tau)$  were examined in Ref. [25] and [26]. The decay channel  $H^+ \rightarrow hW^+$  (which is highly suppressed in natSUSY) was examined in Ref. [27]. The use of three [28] and four [29]  $b$ -quark tags in  $gg \rightarrow tbH^\pm$  was examined. Corrections to the  $tbH^\pm$  vertex were examined in Ref. [30]. Initial projections of the LHC reach for (charged) SUSY Higgs bosons were given by Denegri *et al.* [31] and by Assamagan *et al.* [32]. Search limits from LHC for the  $H^\pm \rightarrow \tau\nu_\tau$  decay mode were presented based on  $\sim 36 \text{ fb}^{-1}$  of integrated luminosity by ATLAS [33] and by CMS [34]. An ATLAS search for charged Higgs bosons in the  $H^\pm tb$  mode based on  $139 \text{ fb}^{-1}$  was given in Ref. [35]. A guidebook for LHC searches for SUSY and non-SUSY charged Higgs bosons was provided in Ref. [36] and a review of non-SUSY charged Higgs is available in Ref. [37].

## 2 A natural SUSY benchmark point and the $m_h^{125}(\text{nat})$ scenario

Following our previous work, we here adopt the same natural SUSY benchmark point as in Ref. [3], which was dubbed  $m_h^{125}(\text{nat})$  since the value of  $m_h$  is very close to its measured value throughout the entire  $m_A$  vs.  $\tan\beta$  plane. We use the two-extra-parameter non-universal Higgs model (NUHM2) [38] with parameter space  $m_0$ ,  $m_{1/2}$ ,  $A_0$ ,  $\tan\beta$ ,  $\mu$ ,  $m_A$  which is convenient for naturalness studies since  $\mu$  can be set to its natural range of  $\mu \sim 100 - 350$  GeV whilst both  $m_A$  and  $\tan\beta$  are free parameters.<sup>2</sup> We adopt the following natural SUSY benchmark Higgs search scenario:

$$m_h^{125}(\text{nat}) : m_0 = 5 \text{ TeV}, m_{1/2} = 1 \text{ TeV}, A_0 = -1.6m_0, \tan\beta, \mu = 200 \text{ GeV and } m_A. \quad (5)$$

A similar  $m_h^{125}(\text{nat})$  benchmark model spectrum, but with  $\mu = 250$  GeV and  $m_{1/2} = 1.2$  TeV, was shown in Table 1 of Ref. [2] for  $\tan\beta = 10$  and  $m_A = 2$  TeV and so for brevity

---

<sup>2</sup>The NUHM2 framework allows for independent soft SUSY breaking mass parameters for the scalar fields  $H_u$  and  $H_d$  in the Higgs sector, but leaves the matter scalar mass parameters universal to avoid flavour problems. The parameters  $m_{H_u}^2$  and  $m_{H_d}^2$  are then traded for  $\mu$  and  $m_A$  in the parameter set shown in (5).

we do not show the revised spectrum here. We adopt the computer code Isajet [39] featuring Isasugra [40] for spectrum generation. The SUSY Higgs boson masses are computed using renormalization-group (RG) improved third generation fermion/sfermion loop corrections [41]. The RG improved Yukawa couplings include full threshold corrections [42] which account for leading two-loop effects [43]. For  $\tan\beta = 10$  and  $m_A = 2$  TeV, we note that  $\Delta_{EW} = 16$  so the model is indeed EW natural. Also, with  $m_h = 124.6$  GeV,  $m_{\tilde{g}} = 2.4$  TeV and  $m_{\tilde{t}_1} = 1.6$  TeV, it is consistent with LHC Run 2 SUSY search constraints. Most important for our purpose, the two lightest neutralinos,  $\tilde{\chi}_1^0$  and  $\tilde{\chi}_2^0$ , and the lighter chargino,  $\tilde{\chi}_1^\pm$ , are higgsino-like with masses  $\sim 200$  GeV while the neutralino  $\tilde{\chi}_3^0$  is bino-like with a mass of 450 GeV and the heaviest neutralino and the heavier chargino have masses  $\sim 0.86$  TeV. Thus, the  $H, A, H^\pm \rightarrow \text{wino} + \text{higgsino}$  decay modes turn on for  $m_{H,A,H^\pm} \gtrsim 1.1$  TeV (although  $H, A, H^\pm \rightarrow \text{bino} + \text{higgsino}$  turns on at somewhat lower  $m_A$  values). It is important to note that while the value of  $\Delta_{EW}$  may change somewhat for small variations of the parameters that are held fixed in Eq. (5), we expect that the Higgs sector phenomenology is relatively insensitive to our specific choice (as long as  $\mu \lesssim 300$  GeV to maintain naturalness).

### 3 $H^\pm$ production cross sections at LHC14

In Fig. 1, we show leading order total cross sections for production of charged SUSY Higgs bosons at LHC14, as generated using Pythia [44] for two values of  $\tan\beta = 10$  (solid) and 40 (dashed). We show cross sections for charged Higgs boson production at the LHC via  $tH^\pm$  production (blue), resonant  $H^\pm$  production (light green),  $H^+H^-$  production (light blue), and  $hH^\pm$  (magenta),  $AH^\pm$  (green) and  $HH^\pm$  (red) production.

We see from Fig. 1 that the dominant production mechanism at LHC14 is via the  $gb \rightarrow tH^\pm$  subprocess [13–15]. For  $\tan\beta = 40$ , the cross section varies from  $\sim 10^3$  fb at low  $m_{H^\pm}$  to  $\sim 10^{-2}$  fb at  $m_{H^\pm} \sim 3$  TeV. These dominant cross sections are enhanced by large  $\tan\beta$ . If we compare  $tH^\pm$  production to the rate for  $b\bar{b}, gg \rightarrow A, H$  production [2] for  $\tan\beta = 10$  and  $m_A \sim 1.5$  TeV, we find that charged Higgs production rates are suppressed compared to resonance production of  $A$  by a factor  $\sim 5$ . And since  $\sigma(b\bar{b}, gg \rightarrow A) \sim \sigma(b\bar{b}, gg \rightarrow H)$ , charged Higgs production compared to resonance  $H, A$  production is suppressed by about an order of magnitude. This seems reasonable since charged Higgs production occurs in association with a (spectator) top quark in contrast to the resonantly produced neutral  $H$  or  $A$  boson.

The next largest cross section is direct resonance production of  $H^\pm$  via (Yukawa suppressed)  $u\bar{d}$  fusion or via (parton distribution function suppressed)  $c\bar{s}$  fusion. Note that this is suppressed relative to neutral  $H/A$  resonance production from  $b\bar{b}$  fusion by the smaller Yukawa couplings (of the first two generation of quarks) and/or small Kobayashi Maskawa mixing elements. These light green curves show a  $\tan\beta$  enhancement due to the Yukawa couplings involved in the production mechanism. The resonance production cross section is typically about two orders of magnitude below  $tH^\pm$  associated production.

The next largest production cross sections are  $HH^\pm$  and  $AH^\pm$  which are produced via  $W^*$  exchange followed closely by  $H^+H^-$  pair production which takes place via  $s$ -channel  $\gamma^*$  and  $Z^*$  exchange. All these production vertices involve gauge interactions and so are  $\tan\beta$  independent. As a result, the  $\tan\beta = 10$  and 40 curves lie on top of one another. These three cross sections

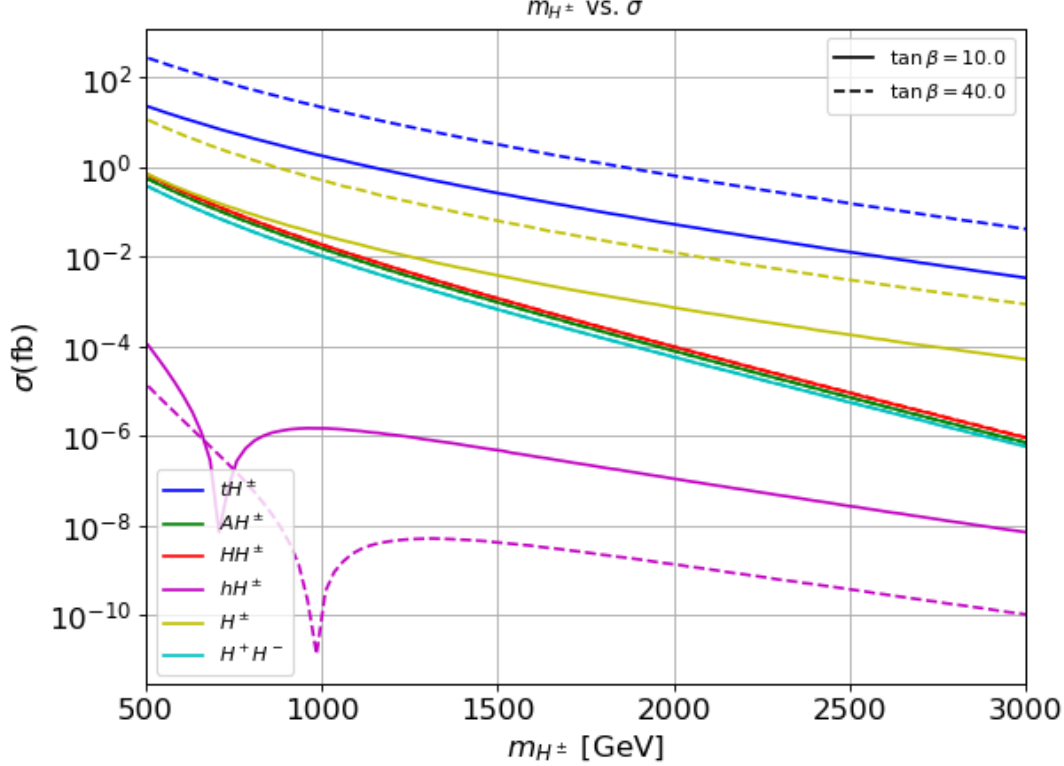


Figure 1: The total cross section for  $pp \rightarrow H^\pm + X$  via various production mechanisms at LHC14 for  $\tan \beta = 10$  (solid) and  $\tan \beta = 40$  (dashed).

are kinematically suppressed because they involve the production of a pair of heavy bosons, and are  $\sim 1.5 - 3$  orders of magnitude below the dominant  $tH^\pm$  cross sections.

In magenta, we show  $hH^\pm$  associated production which occurs dominantly via  $s$ -channel  $W^*$  exchange where the production vertex includes a factor  $g \cos(\alpha + \beta)$  (see Eq. (8.110) of Ref. [1])<sup>3</sup> which vanishes in the decoupling limit. As a result, these cross sections are suppressed from the dominant  $tH^\pm$  cross section by  $\sim 3 - 5$  orders of magnitude depending on  $m_{H^\pm}$  and  $\tan \beta$ . They also feature a dip at certain values of  $m_{H^\pm}$  which occurs when the Higgs mixing angle  $\alpha$  is such that  $\cos(\alpha + \beta) \rightarrow 0$ . An additional cross section  $\sigma(pp \rightarrow W^\pm H^\mp + X)$  occurs at the loop level, and so is highly suppressed and we do not include it here: see Ref. [45].

In light of our discussion of the various production cross sections, for our HL-LHC SUSY charged Higgs reach analysis we will restrict ourselves to the dominant  $tH^\pm$  production process. In Fig. 2 we show the values of  $\sigma(pp \rightarrow tH^\pm + X)$  at LHC14 in the  $m_A$  vs.  $\tan \beta$  plane for our  $m_h^{125}(\text{nat})$  scenario. The largest cross sections  $\sim 10^3$  fb are denoted by dark red whilst the lowest cross sections  $\sim 10^{-3}$  fb are denoted dark blue. We also show the latest ATLAS 95% CL exclusion limit from their search for  $H, A \rightarrow \tau^+ \tau^-$  events using LHC13 with  $139 \text{ fb}^{-1}$  in

<sup>3</sup>The convention for Higgs mixing angle  $\alpha$  in Ref. [1] differs from often-used conventions which result in the mixing angle factor  $\cos(\alpha - \beta)$ .

several non-natural Higgs scenarios which nonetheless maintain  $m_h \sim 125$  GeV [46]. Thus, to uncover new physics at HL-LHC in the SUSY Higgs sector, we will mainly focus our attention on  $m_{H^\pm}$  values in the TeV range.

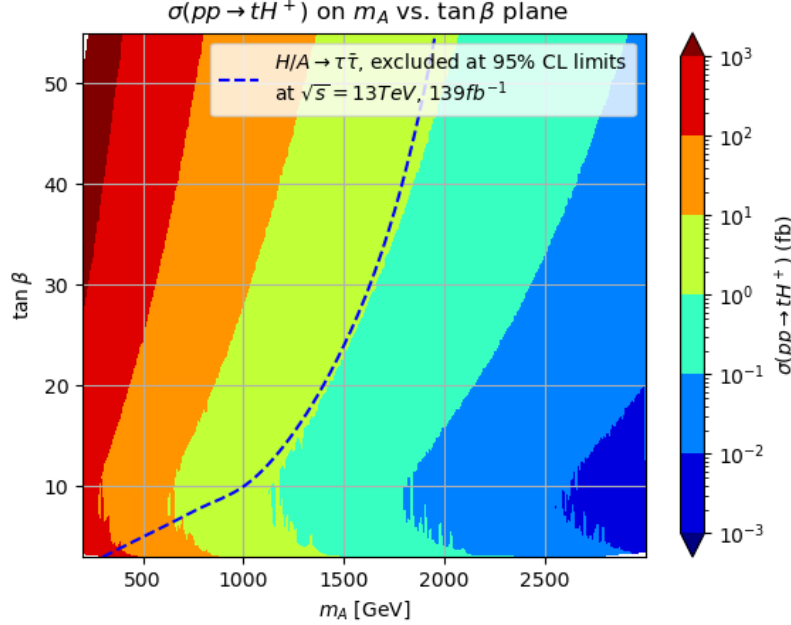


Figure 2: The dominant  $pp \rightarrow tH^\pm + X$  cross section at  $\sqrt{s} = 14$  TeV in the  $m_A$  vs.  $\tan \beta$  plane. The region to the left of the dashed blue line, is currently excluded at the 95% confidence level by limits from ATLAS searches for  $pp \rightarrow H$ ,  $A \rightarrow \tau^+\tau^-$  [46].

## 4 $H^\pm$ branching fractions in natSUSY

The LHC signal from charged Higgs boson production will clearly depend on how  $H^\pm$  decays. For TeV scale values of  $m_{H^\pm}$ , the dominant SM decays are via  $H^\pm \rightarrow tb$  and  $H^\pm \rightarrow \tau\nu_\tau$ . Decays to  $h$ ,  $W$  and  $Z$  bosons are dynamically suppressed. Charged Higgs boson decays via the gaugino plus higgsino modes can also be important if these are not kinematically suppressed. With this in mind, in Fig. 3, we show some select  $H^\pm$  branching fractions (BFs) in the  $m_A$  vs.  $\tan \beta$  plane for the model plane (Eq. 5). The branching fractions are color-coded, with the larger ones denoted by red whilst the smallest ones are denoted by dark blue. The branching fractions are extracted from the Isasugra code [39].

In Fig. 3a) we show the BF for  $H^+ \rightarrow t\bar{b}$ . This decay mode to SM particles is indeed dominant for  $m_A \lesssim 1$  TeV and for larger values of  $\tan \beta \gtrsim 20 - 30$ . In frame b), we show the  $\text{BF}(H^+ \rightarrow \tau^+\nu_\tau)$ . Like  $H^+ \rightarrow t\bar{b}$ , this mode is enhanced at large  $\tan \beta$  and has provided the best avenue for SUSY charged Higgs discovery/exclusion plots so far.

While SUSY decay modes of  $H^\pm$  to higgsino pairs are also open in these regions, these decay modes are suppressed by mixing angles for reasons discussed below. Supersymmetry requires

that there is a direct gauge coupling [1]

$$\mathcal{L} \ni -\sqrt{2} \sum_{i,A} \mathcal{S}_i^\dagger g t_A \bar{\lambda}_A \psi_i + H.c. \quad (6)$$

where  $\mathcal{S}_i$  labels various matter and Higgs scalar fields of the MSSM,  $\psi_i$  is the fermionic superpartner of  $\mathcal{S}_i$  and  $\lambda_A$  is the gaugino with gauge index  $A$ . Also,  $g$  is the corresponding gauge coupling for the gauge group in question and the  $t_A$  are the corresponding gauge group matrices. Letting  $\mathcal{S}_i$  be the Higgs scalar fields, we see there is an unsuppressed coupling of the Higgs scalars to a gaugino and a higgsino as mentioned earlier. This coupling can lead to dominant SUSY Higgs boson decays to SUSY particles when the gaugino-plus-higgsino decay channel is kinematically unsuppressed. But it also shows why the heavy Higgs decay to higgsino pairs is suppressed by mixing angles for  $|\mu| \ll |M_{1,2}|$ , once we recognize that a Higgs boson-higgsino-higgsino coupling is forbidden by gauge invariance.

In frame *c*), we show  $\text{BF}(H^+ \rightarrow \tilde{\chi}_1^0 \tilde{\chi}_2^+)$ , where  $\tilde{\chi}_1^0$  is dominantly higgsino-like and  $\tilde{\chi}_2^+$  is dominantly wino-like for natural SUSY models like the  $m_h^{125}(\text{nat})$  scenario. Here, we see that for larger values of  $m_A \simeq m_{H^\pm} \gtrsim 1.2$  TeV, then this mode turns on, and at least for moderate  $\tan \beta \sim 10 - 20$  (which is favored by naturalness [12]), rapidly comes to dominate the  $H^+$  decay modes along with the neutral wino+higgsino channels  $H \rightarrow \tilde{\chi}_2^+ \tilde{\chi}_2^0$  (frame *d*)) and  $H^+ \rightarrow \tilde{\chi}_1^+ \tilde{\chi}_4^0$  (frame *e*)). In our analysis we have assumed that the gaugino mass parameters unify at the high scale, so that at the weak scale  $M_1 \simeq \frac{1}{2} M_2$ : as a result,  $\chi_3^0$  is dominantly bino-like,  $\chi_4^0$  and  $\chi_2^\pm$  are dominantly wino-like, while  $\tilde{\chi}_{1,2}^0$  and  $\chi_1^\pm$  are mainly higgsino-like. The sum of these three wino+higgsino decay channels thus dominate the  $H^+$  decay branching fractions for  $m_{H,A} \gtrsim 1.2$  TeV and low-to-moderate values of  $\tan \beta$ . For high values of  $\tan \beta$ , the  $b$  and  $\tau$  Yukawa couplings become large, and SM decays to fermions once again dominate SUSY decays. Decays of  $H^+$  to gauge boson pairs and to  $h$  are unimportant in the decoupling limit as mentioned above. For completeness, we also show in frame *f*) the decay mode  $H \rightarrow \tilde{\chi}_1^+ \tilde{\chi}_3^0$  which is to higgsino+bino. This mode is large only in a small region of  $m_H \sim 1$  TeV and modest  $\tan \beta$  where the mode  $H \rightarrow \text{bino} + \text{higgsino}$  decay has turned on, but where  $H \rightarrow \text{wino} + \text{higgsino}$  has yet to become kinematically open. Decays to winos dominate decays to binos because the  $SU(2)$  gauge coupling  $g$  is larger than the hypercharge gauge coupling  $g'$ .

## 5 Search for $H^\pm \rightarrow \tau \nu_\tau$

Next, we turn to the examination of the prospects for discovering the charged Higgs boson produced at the HL-LHC via  $pp \rightarrow H^\pm t + X$ , followed by  $H^\pm \rightarrow \tau \nu_\tau$  decay. For signal and  $2 \rightarrow 2$  background processes listed below, we use the Pythia event generator [44]. For  $2 \rightarrow 3$  BG processes such as  $Wb\bar{b}$ ,  $Zb\bar{b}$  and  $ht\bar{t}$  production, we adopt Madgraph [47] for the subprocess calculation but then interface with Pythia for parton showers, hadronization and underlying event. Our final state particles are then fed into the Delphes [48] detector simulation program which includes a jet-finding algorithm and routines for identifying both  $b$ -jets and hadronic tau jets (labelled as  $\tau_h$ ).

In Delphes, a jet object is reconstructed using an anti- $k$  algorithm with  $p_T(\text{min}) > 25$  GeV and  $\Delta R < 0.4$ . For a baseline jet we require:



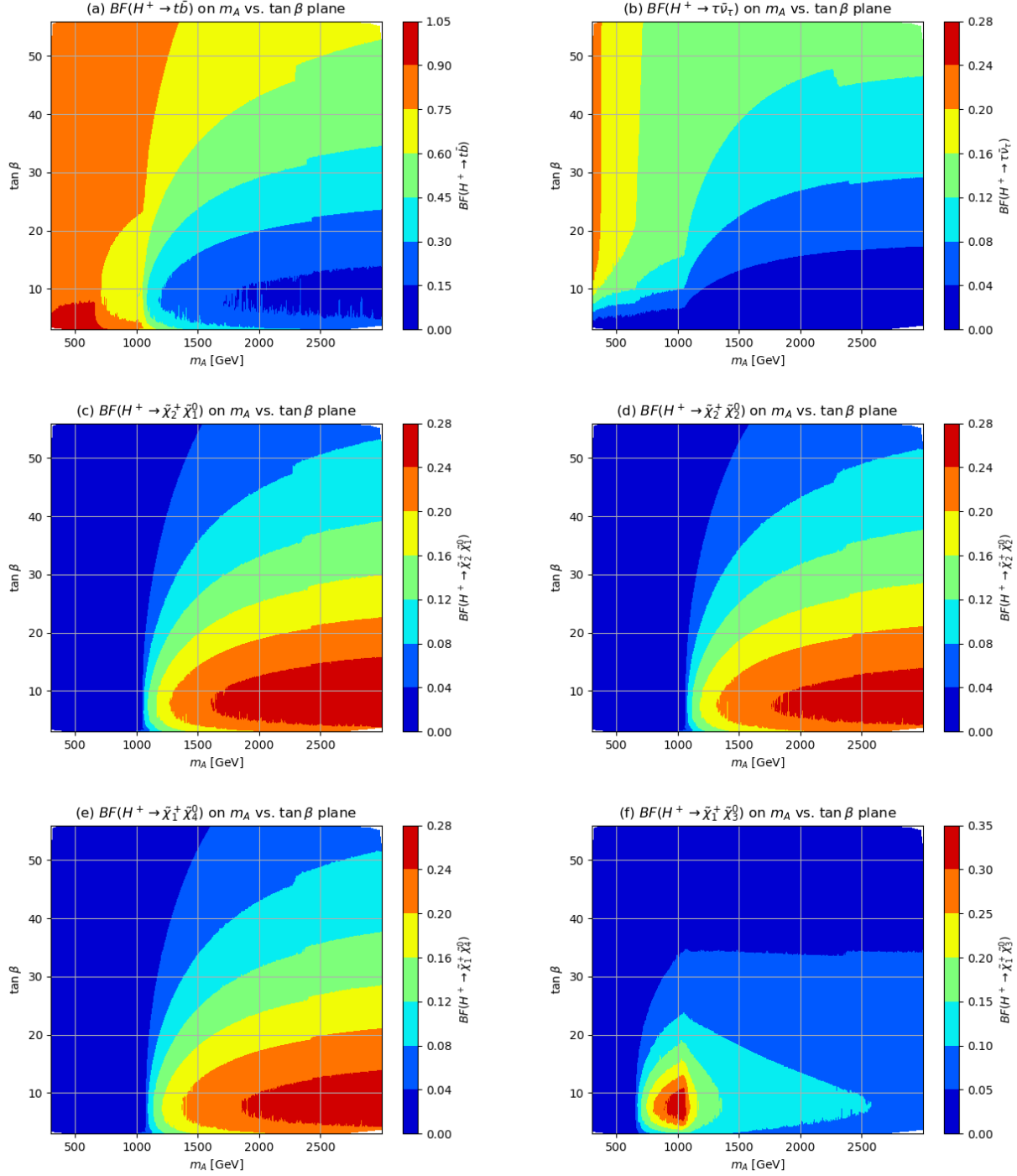


Figure 3: Branching fractions in the  $m_A$  vs.  $\tan \beta$  plane for  $H^+$  to a)  $t\bar{b}$ , b)  $\tau^+\nu_\tau$ , c)  $\tilde{\chi}_2^+\tilde{\chi}_1^0$ , d)  $\tilde{\chi}_2^+\tilde{\chi}_2^0$ , e)  $\tilde{\chi}_1^+\tilde{\chi}_4^0$  and f)  $\tilde{\chi}_1^+\tilde{\chi}_3^0$  from Isajet 7.88 [39] for the model line introduced in the text.

- $|\eta(j)| < 4.7$ .

For a baseline  $b$ -jet, besides the requirement for a baseline jet, we further require

- the jet to be tagged as a  $b$ -jet by Delphes.

For a signal  $\tau_h$ -jet, besides the requirement of baseline jet, we further require

- the jet must be a tagged hadronic tau-jet  $\tau_h$  by Delphes with
- $|\eta(\tau_h)| < 2.5$ .

For the baseline lepton isolation requirement, we require

- $p_T(\min)(e/\mu) > 5 \text{ GeV}$ .

For a signal lepton, besides the requirement for baseline lepton isolation, we further require

- $|\eta_{e,(\mu)}| < 2.47 \text{ (2.5)}$  and
- $p_T(e(\mu)) > 20 \text{ (25)} \text{ GeV}$ .

## 5.1 $H^\pm \rightarrow \tau\nu_\tau \rightarrow \tau_h + \cancel{E}_T$ channel

In this channel, we search for  $H^\pm \rightarrow \tau_h + \cancel{E}_T$  along with the presence of a spectator  $t$ -jet which is signalled by the presence of a tagged  $b$ -jet. We include SM BGs from  $t\bar{t}$ , single top,  $Wb\bar{b}$ ,  $Zb\bar{b}$ ,  $WW$ ,  $WZ$ ,  $ZZ$ ,  $Zh$ ,  $Wh$  and  $ht\bar{t}$  production. We first require:

- exactly one signal  $\tau_h$ -jet with no baseline leptons; the no baseline lepton requirement targets events where the spectator top decays hadronically, though of course events with a semileptonic decaying top could contribute if the lepton evades detection;
- $n(b\text{-jet}) \geq 1$ , where  $b$  here (and in the rest of Sec. 5) refers to baseline  $b$ -jets, and
- a neutrino reconstruction method<sup>4</sup> is employed here. If the invariant mass of the reconstructed neutrino, the signal  $\tau_h$ -jet and any of the tagged baseline  $b$ -jets in the event reconstructs to  $m = m_t \pm 50 \text{ GeV}$ , then the event is vetoed.

This latter requirement is imposed to veto a portion of the very large  $pp \rightarrow t\bar{t}$  background.

With these remaining events, an examination of various distributions of signal and background (that we do not show for brevity) leads us to impose the following analysis cuts:

- $\cancel{E}_T > 350 \text{ GeV}$ ,
- $\Delta\phi(\tau_h, \vec{\cancel{E}}_T) > 30^\circ$ ,
- $\Delta\phi(b_1, \vec{\cancel{E}}_T) > 50^\circ$ , where  $b_1$  is the leading baseline  $b$ -jet, and

---

<sup>4</sup>In  $t\bar{t}$  events where one of the tops decays hadronically, and the other leptonically, so that the  $\cancel{E}_T$  comes only from the (massless) neutrino; i.e.  $\cancel{E}_{T,x,y} = p(\nu)_{x,y}$ , one can construct  $p(\nu)_z$  assuming that the  $W$  boson from top decay is on-shell. This vetoes about half the potentially enormous  $t\bar{t}$  background with a loss of less than 10% of the signal.

- $\min(\Delta R(b, \tau_h)) > 0.9$ , where the  $b$  loops over all tagged baseline  $b$ -jets in the event.

After these cuts, the resulting transverse mass distribution  $m_T(\tau_h, \cancel{E}_T)$  is shown in Fig. 4. As expected, the signal histograms peak around the value of  $m_{H^\pm}$ , while the backgrounds yield falling distributions. Our goal in each signal channel is to look for an excess above the SM backgrounds in the largest transverse mass bins which are most sensitive to TeV-scale charged Higgs decay. From the distribution, the solid colored histograms represent the various BGs, of which the dominant is light yellow:  $t\bar{t}$ . The signal distributions, labelled as dotted curves for several benchmark scenarios as listed, can emerge from BG at large values of  $m_T$ , provided the signal is large enough.

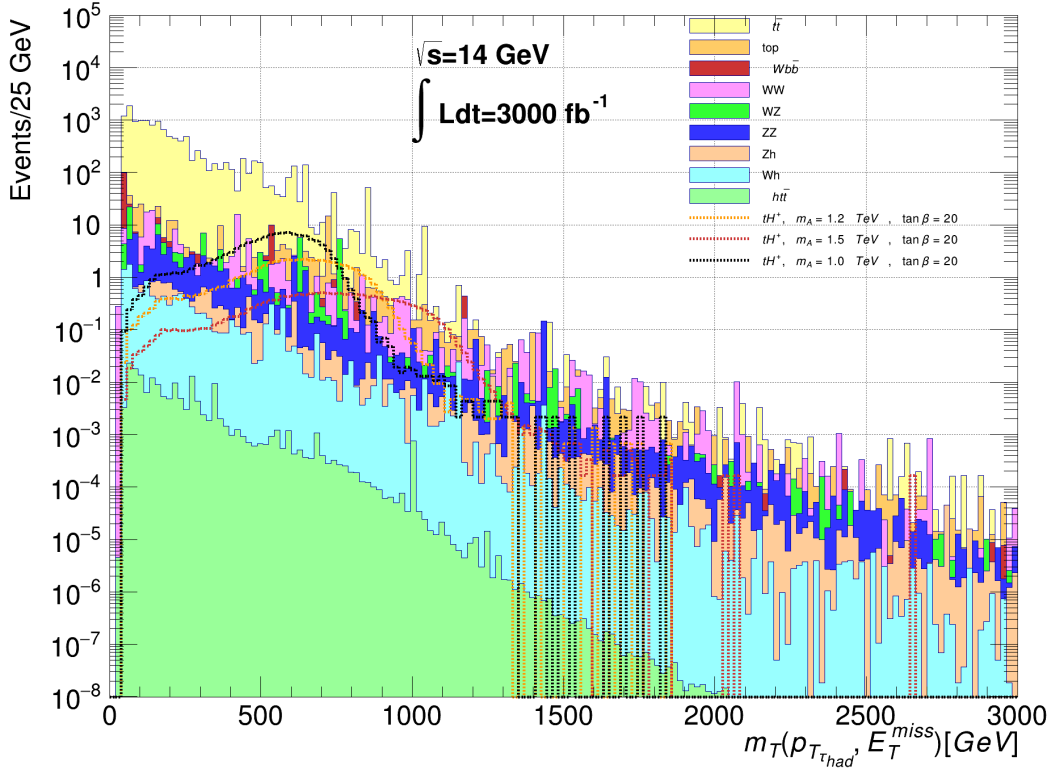


Figure 4: Distribution in  $m_T(\tau_h, \cancel{E}_T)$  from  $pp \rightarrow H^\pm(\rightarrow \tau\nu) + t + X$  followed by the decay  $\tau \rightarrow \text{hadrons} + \cancel{E}_T$ . We also show dominant SM backgrounds.

## 5.2 $H^\pm \rightarrow \tau\nu_\tau \rightarrow \ell + \cancel{E}_T$ channel

In this subsection, we examine the  $pp \rightarrow tH^\pm + X$  production reaction where  $H^\pm \rightarrow \tau\nu_\tau$  followed by  $\tau \rightarrow \nu_\tau + (\ell\nu_\ell)$  channel, where  $\ell = e$  or  $\mu$ . For this signal channel, we require:

- exactly one signal lepton and no other baseline leptons,

- no jets have been  $\tau$ -tagged ( $\tau_h$ -veto); here, we are again targeting events where the top decays hadronically, and the tau decays leptonically.
- $n(b - \text{jet}) \geq 1$  and
- the neutrino reconstruction method described above is employed here. If the invariant mass of the reconstructed neutrino, the signal lepton plus any of the baseline  $b$ -jets in the event is within  $m = m_t \pm 50$  GeV, then event is vetoed.

Standard Model backgrounds from  $t\bar{t}$ , single top,  $Wb\bar{b}$ ,  $WW$ ,  $WZ$ ,  $Wh$ ,  $ht\bar{t}$  and  $Zh$  can also lead to the same event topology as the signal.

Examination of various distributions leads us to impose the following analysis cuts:

- $E_T > 350$  GeV,
- $E_{T,rel} := E_T \cdot \sin(\min(\Delta\phi, \frac{\pi}{2})) > 150$  GeV, where  $\Delta\phi$  is the azimuthal angle between the  $\vec{E}_T$  and the closest lepton or jet with  $p_T > 25$  GeV.
- $\Delta\phi(\ell, \vec{E}_T) > 30^\circ$ ,
- $\Delta\phi(b_1, \vec{E}_T) > 70^\circ$ , where  $b_1$  is the leading baseline  $b$ -jet and
- $\min(\Delta R(b, \ell)) > 1.2$ , where the  $b$  loops over all tagged baseline  $b$ -jets in the event.

The resultant  $m_T(\ell, \vec{E}_T)$  distribution is displayed in Fig. 5. The dominant BG at low  $m_T$  comes from  $t\bar{t}$  production (light-yellow histogram) while the dominant BG at high  $m_T$  comes from  $WW$  production. We also show several signal benchmark distributions (dotted curves) which may cause an excess of events over background expectations at high  $m_T(\ell, \vec{E}_T)$ . In this case, the signal distributions shown will only cause a slight excess above background at high  $m_T$ . But combined with the other channels, this signal channel can slightly increase the overall significance.

### 5.3 $H^\pm \rightarrow \tau\nu_\tau$ with $t \rightarrow b\ell\nu_\ell$ channel

In this channel, we attempt to extract the signal from  $pp \rightarrow tH^\pm$  production followed by  $H^\pm \rightarrow \tau_h + \cancel{E}_T$  but where the spectator  $t$ -quark decays semi-leptonically:  $t \rightarrow b\ell\nu_\ell$ . SM backgrounds from  $t\bar{t}$ , single top,  $WW$ ,  $WZ$ ,  $Wh$ ,  $Zh$  and  $ht\bar{t}$  production are included in our analysis.

We require:

- exactly one signal lepton and no other baseline leptons,
- exactly one signal  $\tau_h$ -jet,
- the charges of the signal lepton and the  $\tau_h$ -jet must be OS (opposite-sign) and
- $n(b - \text{jet}) \geq 1$ .

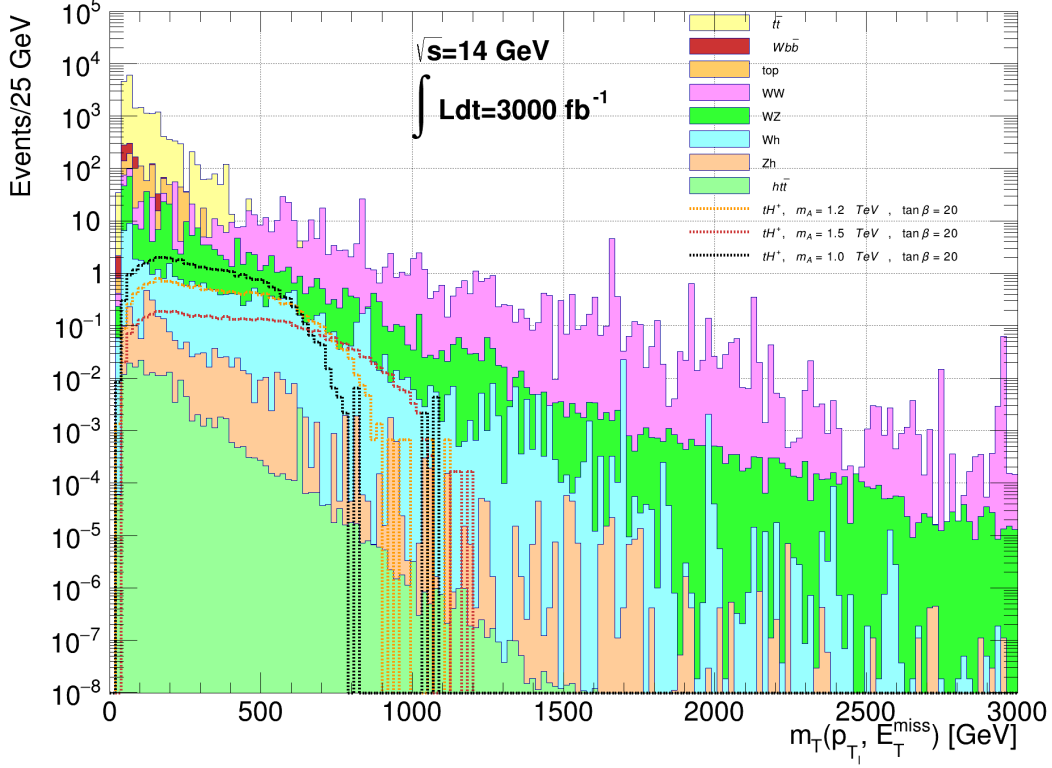


Figure 5: Distribution in  $m_T(\ell, \cancel{E}_T)$  from  $pp \rightarrow H^\pm(\tau\nu) + t + X$  followed by  $\tau \rightarrow \ell + \cancel{E}_T$  decay. We also show dominant SM backgrounds.

Examination of the resultant signal and background distributions leads us to the following additional analysis cuts:

- $\cancel{E}_T > 350$  GeV,
- $\cancel{E}_{Trel} > 150$  GeV,
- $\Delta\phi(\ell, \vec{\cancel{E}}_T) > 20^\circ$ ,
- $\Delta\phi(\tau_h, \vec{\cancel{E}}_T) > 80^\circ$ ,
- $\Delta\phi(b_1, \vec{\cancel{E}}_T) > 50^\circ$ , where  $b_1$  is the leading baseline  $b$ -jet and
- $\min(\Delta R(b, \tau_h)) > 1.2$ , where the  $b$  loops over all baseline  $b$ -jets in the event.

The resultant  $m_T(\tau_h, \cancel{E}_T)$  distribution is shown in Fig. 6. The dominant BG at low  $m_T$  again comes from  $t\bar{t}$  production. At high  $m_T$ , then the various signal histograms can cause a noticeable increase in the expected  $m_T$  distribution beyond SM expectations, albeit with a rather low event rate.

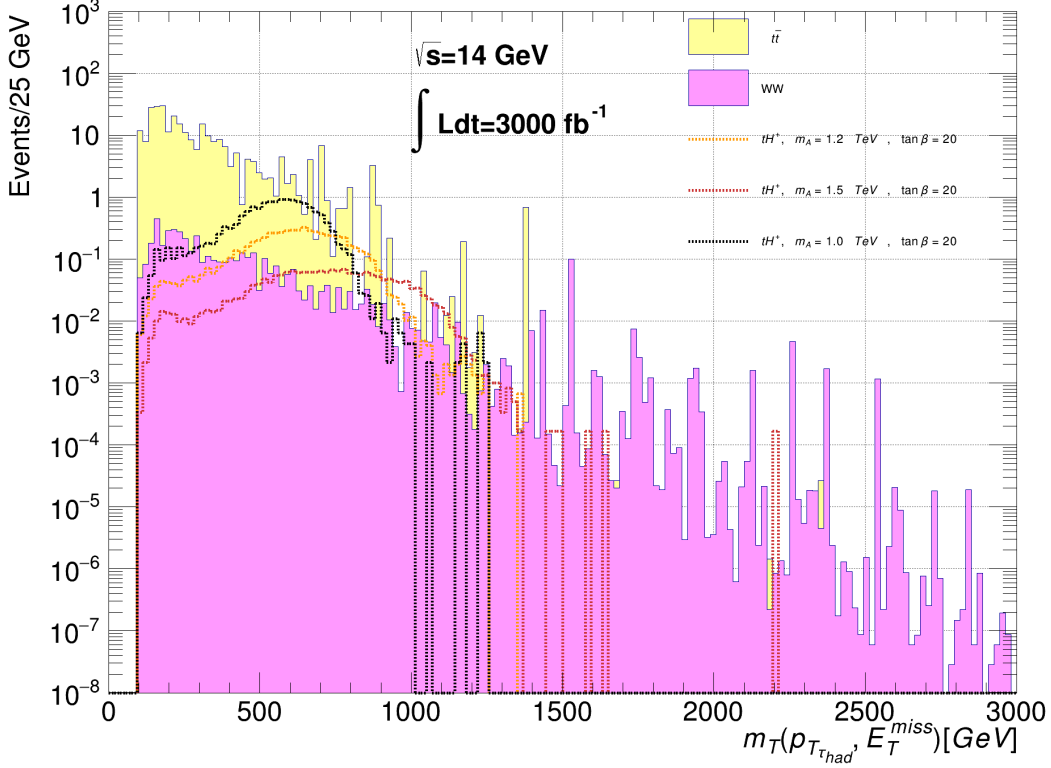


Figure 6: Distribution in  $m_T(\tau_h, \cancel{E}_T)$  from  $pp \rightarrow H^\pm t + X$  followed by  $H^\pm \rightarrow \tau_h + \cancel{E}_T$  decay and also  $t \rightarrow b\ell\nu_\ell$  decay. We also show dominant SM backgrounds.

#### 5.4 LHC reach in $H^\pm \rightarrow \tau\nu_\tau$ channel

Using the analysis cuts for the various signal channels delineated above, we can now create reach plots to show the LHC14 discovery sensitivity or exclusion limits for  $pp \rightarrow H^\pm t$  production in the  $m_A$  vs.  $\tan\beta$  plane. We use the  $5\sigma$  level to claim discovery of a charged Higgs boson and assume the true distribution one observes experimentally corresponds to signal-plus-background. We then test this against the background-only distribution in order to see if the background-only hypothesis can be rejected at the  $5\sigma$  level. Specifically, we use the binned transverse mass distributions (bin width of 25 GeV) from each signal channel as displayed above to obtain the discovery/exclusion limits.

In the case of the exclusion plane, the upper limits for exclusion of a signal are set at 95% CL; one assumes the true distribution one observes in experiment corresponds to background-only. The limits are then computed using a modified frequentist  $CL_s$  method [49] where the profile likelihood ratio is the test statistic. In both the exclusion and discovery planes, the asymptotic approximation for obtaining the median significance is employed [50].

In Fig. 7, we plot our result for the discovery/exclusion regions via the  $H^\pm \rightarrow \tau\nu$  channel for the HL-LHC with  $\sqrt{s} = 14$  TeV and  $3000 \text{ fb}^{-1}$  of integrated luminosity in the  $m_A$  vs.

$\tan\beta$  plane using our  $m_h^{125}(\text{nat})$  benchmark scenario (which is quite typical for natural SUSY models [51]). In frame *a*), we plot the  $5\sigma$  discovery reach using the combined three channels discussed previously. Above the dashed black line, experiments at the HL-LHC should be able to discover  $H^\pm$  at the LHC operating at  $\sqrt{s} = 14$  TeV, assuming an integrated luminosity of  $3000 \text{ fb}^{-1}$ . The green and yellow bands display the  $\pm 1\sigma$  and  $\pm 2\sigma$  uncertainties in our mapping of the discovery region. The region above the dashed blue line is excluded by ATLAS searches for  $H/A \rightarrow \tau\tau$  events, albeit in a scenario with decoupled superpartners [46]. From the plot, we see that a discovery region does indeed emerge, starting around  $m_A \sim 500$  GeV and  $\tan\beta \sim 18$  and extends out to  $m_A \sim 3$  TeV for  $\tan\beta \sim 50$  where both the  $\sigma(pp \rightarrow tH^\pm + X)$  and the branching fraction for  $H^\pm \rightarrow \tau\nu_\tau$  decays are both enhanced. The discovery region pinches off below  $\tan\beta \sim 15$  where the  $H^\pm \rightarrow \tau\nu_\tau$  branching ratio becomes too small.

In frame *b*), we plot the 95% CL exclusion limit for HL-LHC for our combined three signal channels. The exclusion limit now extends out to beyond  $m_A \sim 3$  TeV for large  $\tan\beta \sim 50$ . We also see that the exclusion contour extends to about  $\tan\beta \sim 10$  for relatively light  $m_{H^\pm}$ ; however, this part of the plane is already excluded by ATLAS searches.

## 6 Search for $H^\pm \rightarrow tb$

In this section, we examine the capability of HL-LHC to discover charged Higgs bosons in the  $H^\pm \rightarrow tb$  decay channel. Recent limits have been placed within this search channel by the ATLAS collaboration using  $139 \text{ fb}^{-1}$  of data [35]. Our analysis proceeds similarly to Sec. 5 except now we place an emphasis on the presence of high- $p_T$  top-jets in the final state.

In the following, we will use lower case letter such as  $j$  ( $b$ ) to denote the small radius jets (tagged  $b$ -jets) while upper case letter such as  $J$  ( $T$ ) denote large radius jets (top-jets).

The parameters for baseline reconstructed particles are, for charged leptons  $l$ :

- $|\eta(e, \mu)| < 4$ ,
- $p_T(e) > 20 \text{ GeV}$ ,  $p_T(\mu) > 25 \text{ GeV}$ .

For small radius jets  $j$ :

- jet reconstruction with the anti- $k_T$  algorithm,
- cone size  $\Delta R < 0.4$ ,
- $p_T(j) > 25 \text{ GeV}$ ,
- $|\eta(j)| < 4.7$ .

For a tagged baseline  $b$ -jet:

- satisfy the above small radius jet requirements,
- tagged  $b$ -jet by Delphes.

For a large radius jet  $J$ :

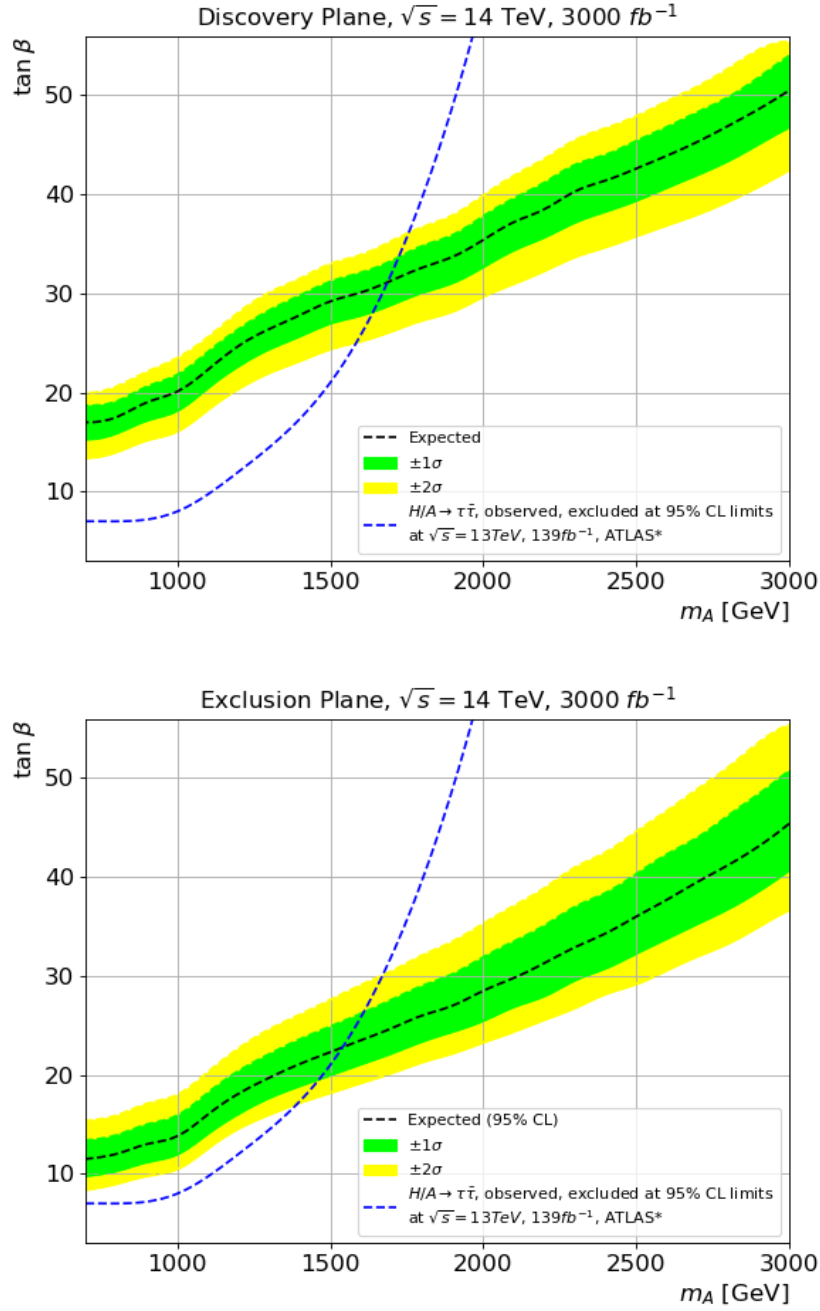


Figure 7: In *a*), we show the 5 $\sigma$  discovery region of the  $m_A$  vs.  $\tan \beta$  plane for  $pp \rightarrow H^{\pm}t + X$  followed by  $\tau \rightarrow \ell + \cancel{E}_T$  decay for HL-LHC with 3000  $\text{fb}^{-1}$ . In *b*), we plot the corresponding 95% CL exclusion region. The region above the dashed blue curve is excluded by ATLAS searches for  $H/A \rightarrow \tau\tau$  events.

- jet reconstruction using the Cambridge/Aachen algorithm (CA) [52, 53],



- cone size  $\Delta R < 1.5$ ,
- $p_T(J) > 300$  GeV and
- $|\eta(J)| < 2$ .

For a tagged top-jet  $T$ :

- satisfy the above large radius jet ( $J$ ) requirements,
- $T$  is tagged by the HEPTopTagger2 algorithm [53, 54].

Also, for candidate events with an isolated lepton or a signal  $b$ -jet, we further require

- $|\eta(e)| < 2.47$ ,  $|\eta(\mu)| < 2.5$  and  $|\eta(b)| < 2.4$ .

The analysis is then separated into four orthogonal channels depending on whether or not the final state does or does not contain a tagged  $T$ -jet, and whether or not it contains an isolated lepton.

In all cases, the small radius  $b$ -jet (denoted as  $b_1$  below) arising directly from the  $H^\pm$  decay is determined by the following procedure.

- we require  $p_T(b_1) > 350$  GeV,
- $|\eta(b_1)| < 1.5$ ,
- $R(b_1, J_1) > 1.5$  (so this means  $b_1$  must be outside the cone of the fat jet top candidate).
- $m(j, j', b_1)$  *cannot* be in the top mass range  $[125, 225]$  GeV, where  $j, j'$  are any small radius jet pairs in the event.
- If multiple candidates satisfying these conditions are found, the one with the hardest  $p_T$  is taken as  $b_1$ .
- Events are vetoed if no  $b$ -jets satisfy these conditions.

Then,  $m(T_1, b_1)$  is used to reconstruct the mass of the  $H^\pm$  in all cases. Note that in the channels where the HEPTopTagger2 has positively tagged a top-jet, *i.e.* the  $1t, 1t1l$  channels, it is the four vector reconstructed by the algorithm that is taken as  $T_1$ . But in the channels where HEPTopTagger2 fails to identify a top-jet, then it is the fat jet itself that is taken as the  $T_1$ . The  $m(T_1, b_1)$  distributions are then shown as the final results for each signal channel.

The background samples being considered for the hadronic channels  $[1t, 1t(\text{no tag})]$  are  $t\bar{t}$  (with  $\geq 3$  truth  $b$ 's removed to avoid double counting with  $t\bar{t}b\bar{b}$  events that are separately simulated), single top,  $t\bar{t}b\bar{b}$  and  $tttt$ . The backgrounds for the semileptonic channels  $[1t1l, 1t(\text{no tag})1l]$  are  $t\bar{t}$  (again with  $\geq 3$  truth  $bs$  removed),  $t\bar{t}b\bar{b}$  and  $t\bar{t}t\bar{t}$ . We have not simulated  $t\bar{t}V$  events as we require at least three  $b$ -jets which has been shown to be very small [55].

## 6.1 Single tagged top channel without signal leptons

In this channel, we search for  $pp \rightarrow tH^\pm + X$  with  $H^\pm \rightarrow tb$  decay. The primary  $t$ -quark in the  $tH^\pm$  final state tends to be non-central, and so rarely produces a tagged top-jet, but does more often produce a tagged  $b$ -jet. So for this channel, we focus on reconstructing the decay-produced top jet from  $H^\pm \rightarrow tb$ , where TeV-scale charged Higgs decay gives rise to a well-collimated  $T$ -jet. Thus,

- The HEPTopTagger2 algorithm that we use has tagged exactly one top from the large radius boosted ( $R < 1.5$ ,  $p_T(J) > 300$  GeV) jet  $n_T = 1$ . (This fat jet is denoted as  $J_1$  below).

The top-jet four vector reconstructed by the HEPTopTagger2 is used as  $T_1$ . The four vector for the subjet  $b$  reconstructed by the tagger is denoted as  $b_2$ . We further require the following.

- At least 3  $b$ -jets:  $n_b \geq 3$ , of which at least two of them must satisfy the signal  $b$ -jet requirements listed above.
- At least 6 jets:  $n_j \geq 6$ .
- No isolated leptons:  $n_l = 0$ .

Based on examination of various signal/background distributions, we also require

- $H_T > 1200$  GeV,
- $m(b, b') > 215$  GeV, where the  $b$  and  $b'$  are the  $b$ -jet pair with the max  $p_T$  in the events,
- $\max(R(b', H^\pm)) > 1.5$ , where the  $b'$  are any  $b$ -jets in events that are not  $b_1$  and  $b_2$ . The  $H^\pm$  is reconstructed from  $T_1$ ,  $b_1$ ,
- $\min(R(b', b_1)) < 2.8$ , where  $b'$  are any  $b$ -jets in the events.

At this point, we are able to construct the distribution  $m(tb) \equiv m(T_1, b_1)$  shown in Fig. 8. The dominant background distributions are shown as solid colored histograms whilst several signal benchmark models are shown as dashed histograms. From the plot, we see that the signal distributions roughly reconstruct  $m(H^\pm)$  while background is dominated by  $t\bar{t}b\bar{b}$  production at low mass, and by  $t\bar{t}$  at high invariant mass. The goal then is to search for resonant signal bumps against the continuum of expected backgrounds. If this bump is buried under the SM background, this channel will make a negligible contribution to the significance when combined with other channels.

## 6.2 Single top (no tag) channel without signal leptons

In this channel, the HEPTopTagger2 fails to tag any tops. However,

- there is at least one large radius boosted ( $R < 1.5$ ,  $p_T > 300$  GeV) jet  $n_J \geq 1$  with trimmed mass [56]  $115 \text{ GeV} < m_J < 190 \text{ GeV}$ , and at least one small radius ( $R < 0.4$ )  $b$ -jet within the cone of the large radius jet  $J$ . Then, the fat Jet with the hardest  $p_T$  is taken as the top candidate arising directly from the charged Higgs decay (denoted as  $J_1/T_1$ ). The hardest  $b$  within  $J_1/T_1$  cone is taken as  $b_2$ .

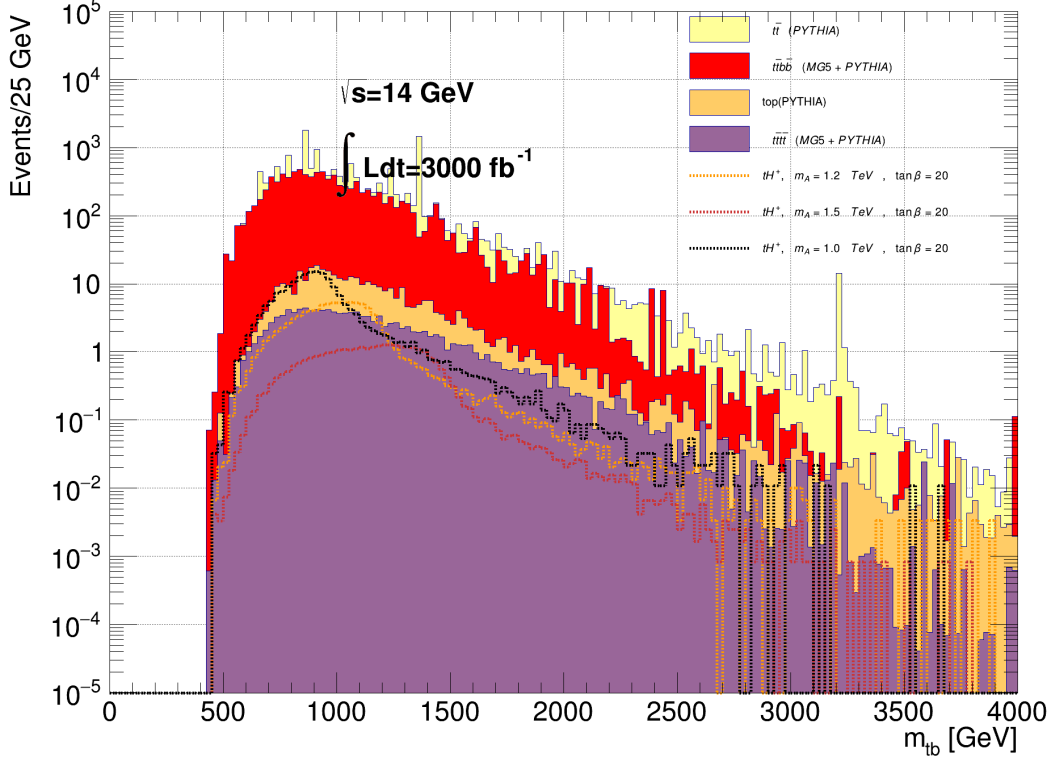


Figure 8: Distribution in  $m(tb)$  from  $pp \rightarrow H^\pm t + X$  followed by  $H^\pm \rightarrow tb$  decay. These events include a top-jet tagged by HEPTopTagger2. We also show dominant SM backgrounds.

- At least 3  $b$  jets:  $n_b \geq 3$ , of which at least two of them must satisfy the signal  $b$ -jet requirements listed above.
- At least 6 jets:  $n_j \geq 6$  and
- No isolated leptons:  $n_l = 0$ .

We then require:

- $H_T > 1200$  GeV,
- $m(b, b') > 215$  GeV, where the  $b, b'$  are the  $b$ -jet pairs with the max  $p_T$  in the events,
- $\max(R(b', H^\pm)) > 2.4$ , where the  $b'$  are any  $b$ -jets in events that are not  $b_1$  and  $b_2$ . The  $H^\pm$  is reconstructed from  $T_1, b_1$ ,
- $0.8 < \min(R(b', b_1)) < 2.8$ , where the  $b'$  are any  $b$ -jets in the events.

The distribution  $m(tb)$ , reconstructed from  $T_1$  and  $b_1$ , is shown in Fig. 9 where again the  $m(tb)$  roughly reconstructs  $m(H^\pm)$  and where again the  $t\bar{t}$  and  $t\bar{t}b\bar{b}$  are the dominant backgrounds.

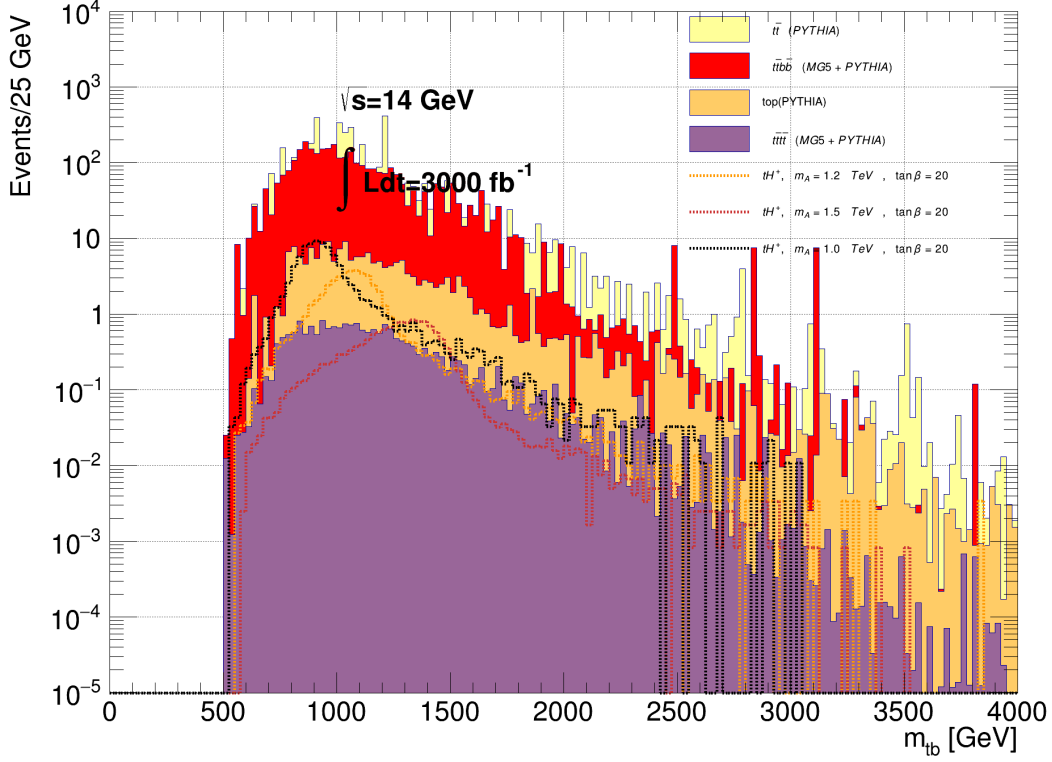


Figure 9: Distribution in  $m(tb)$  from  $pp \rightarrow H^\pm t + X$  followed by  $H^\pm \rightarrow tb$  decay, but no fat jet tagged as top by HEPTopTagger2. We also show dominant SM backgrounds.

### 6.3 Single top (tagged) plus lepton channel

In this signal channel, we again require tagged top-jet, but now also require the presence of an isolated lepton arising from semileptonic decay of one of the tops.

We require

- The HEPTopTagger2 has tagged exactly one top from the large radius boosted ( $R < 1.5$ ,  $p_T > 300$  GeV) jet  $n_T = 1$ .

As before the top four vector reconstructed by the HEPTopTagger2 is denoted as  $T_1$ . The four vector for the subjet  $b$  reconstructed by the tagger is denoted as  $b_2$ .

- At least 3  $b$ -jets:  $n_b \geq 3$ , of which at least two of them must satisfy the signal  $b$ -jet requirements listed above.
- At least 4 jets:  $n_j \geq 4$ .
- Exactly one signal isolated leptons:  $n_l = 1$ .

We further require

- $H_T > 1200$  GeV,
- $m(b, b') > 215$  GeV, where the  $b, b'$  are the  $b$  pairs with the max  $p_T$  in the events,
- $\max(R(b', H^\pm)) > 1.5$ , where  $b'$  are any  $b$ -jets in the events that are not  $b_1$  and  $b_2$ . The  $H^\pm$  is reconstructed from  $T_1$  and  $b_1$ .
- $\min(R(b', b_1)) > 1$ , where the  $b'$  are any  $b$ -jets in the events, and
- $R(b_1, l) > 0.9$ .

The  $m(tb)$  invariant mass distribution from the signal BM models and backgrounds, again constructed by combining  $T_1$  and  $b_1$ , are shown in Fig. 10. In this case, the  $t\bar{t}b\bar{b}$  background is dominant in the range where  $m(tb)$  reconstructs  $m(H^\pm)$ .

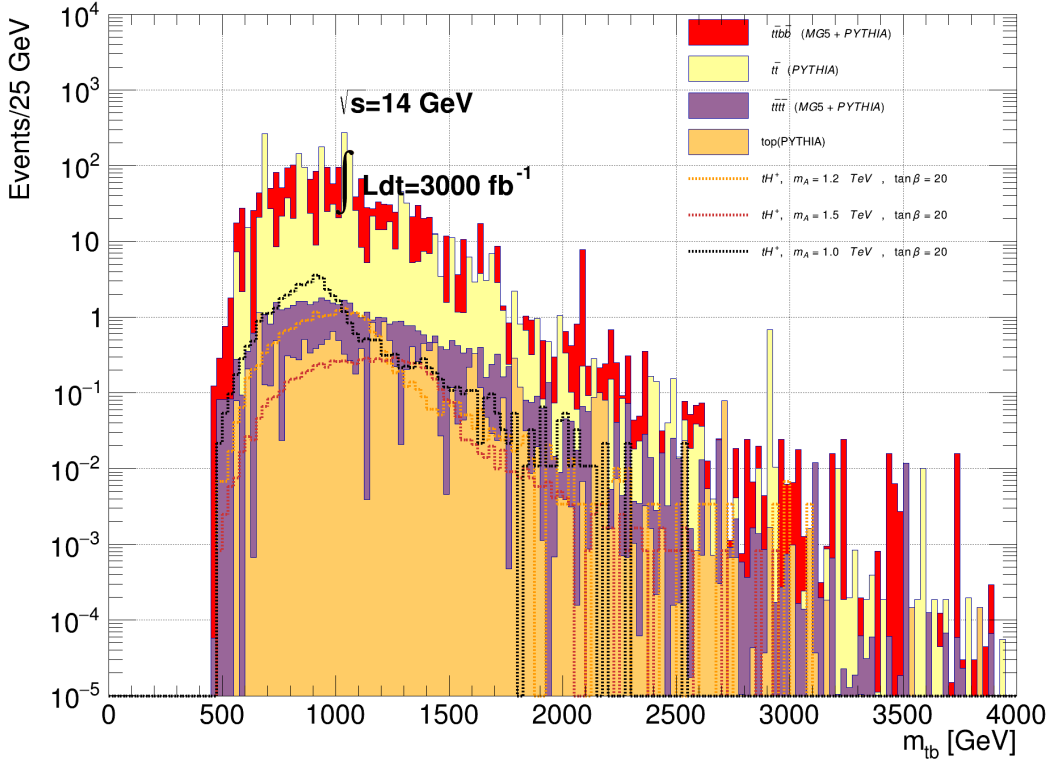


Figure 10: Distribution in  $m(tb)$  from  $pp \rightarrow H^\pm t + X$  followed by  $H^\pm \rightarrow tb$  decay, a fat jet tagged as a top-jet by HEPTopTagger2, and an isolated lepton from the decay of one of the top quarks. We also show dominant SM backgrounds.

## 6.4 Single top (no tag) plus lepton channel

In this channel, we examine events where the HEPTopTagger2 fails to tag any top jets but there is a lepton from the decay of one of the tops. We require,

- there is at least one large radius boosted ( $R < 1.5$ ,  $p_T > 300$  GeV) jet  $n_J \geq 1$  with trimmed mass [56]  $115 \text{ GeV} < m_J < 190 \text{ GeV}$ , and at least one small radius ( $R < 0.4$ )  $b$ -jet within the cone of the large radius jet  $J$ . Then, the fat Jet is taken as the hardest  $p_T$  top candidate directly from the charged Higgs decay (denoted as  $J_1/T_1$ ). The hardest  $b$ -jet within  $J_1/T_1$  is taken as  $b_2$ .
- At least 3  $b$ -jets:  $n_b \geq 3$ , of which at least two of them must satisfy the signal  $b$ -jet requirements listed above.
- At least 6 jets:  $n_j \geq 6$ .
- Exactly one signal isolated lepton:  $n_l = 1$ .

We also require

- $H_T > 1200 \text{ GeV}$ ,
- $m(b, b') > 215 \text{ GeV}$ , where the  $b, b'$  are the  $b$  pairs with the max  $p_T$  in the events,
- $\max(R(b', H^\pm)) > 1.1$ , where  $b'$  are any  $b$ -jets in the events that are not  $b_1$  and  $b_2$ .  $H^\pm$  is reconstructed from  $T_1$  and  $b_1$ ,
- $\min(R(b', b_1)) > 1$ , where  $b'$  are any  $b$ -jets in the events and
- $R(b_1, l) > 0.9$ .

The  $m(tb)$  distribution (again constructed by combining  $T_1$  and  $b_1$ ) for signal and background events with non-tagged top-jets and an isolated lepton is shown in Fig. 11.

## 6.5 LHC reach in $H^\pm \rightarrow tb$ channel

As in the  $H^\pm \rightarrow \tau\nu_\tau$  analysis, after adopting the above cuts for the various signal channels, we can now create reach plots in terms of discovery sensitivity or exclusion limits for  $pp \rightarrow H^\pm t + X$  followed by  $H^\pm \rightarrow tb$  in the  $m_A$  vs.  $\tan\beta$  plane. In this case, we use the binned  $m(tb)$  distributions (bin width of 25 GeV) from each signal channel as displayed above to obtain the discovery/exclusion limits.

In Fig. 12, we show our results for the discovery/exclusion regions via the  $H^\pm \rightarrow tb$  channel for the HL-LHC with  $\sqrt{s} = 14 \text{ TeV}$  and  $3000 \text{ fb}^{-1}$  of integrated luminosity in the  $m_A$  vs.  $\tan\beta$  plane using our  $m_h^{125}(\text{nat})$  benchmark scenario. In frame *a*), we plot the  $5\sigma$  discovery reach using the combined four  $H^\pm \rightarrow tb$  signal channels listed above. The dashed black line denotes the computed reach while the green and yellow bands display the  $\pm 1\sigma$  and  $\pm 2\sigma$  uncertainty. From the plot, we see that a discovery region is indeed found, starting around  $m_A \sim 500 \text{ GeV}$  and  $\tan\beta \sim 18$ . For these combined  $H^\pm \rightarrow tb$  signal channels, the discovery region extends

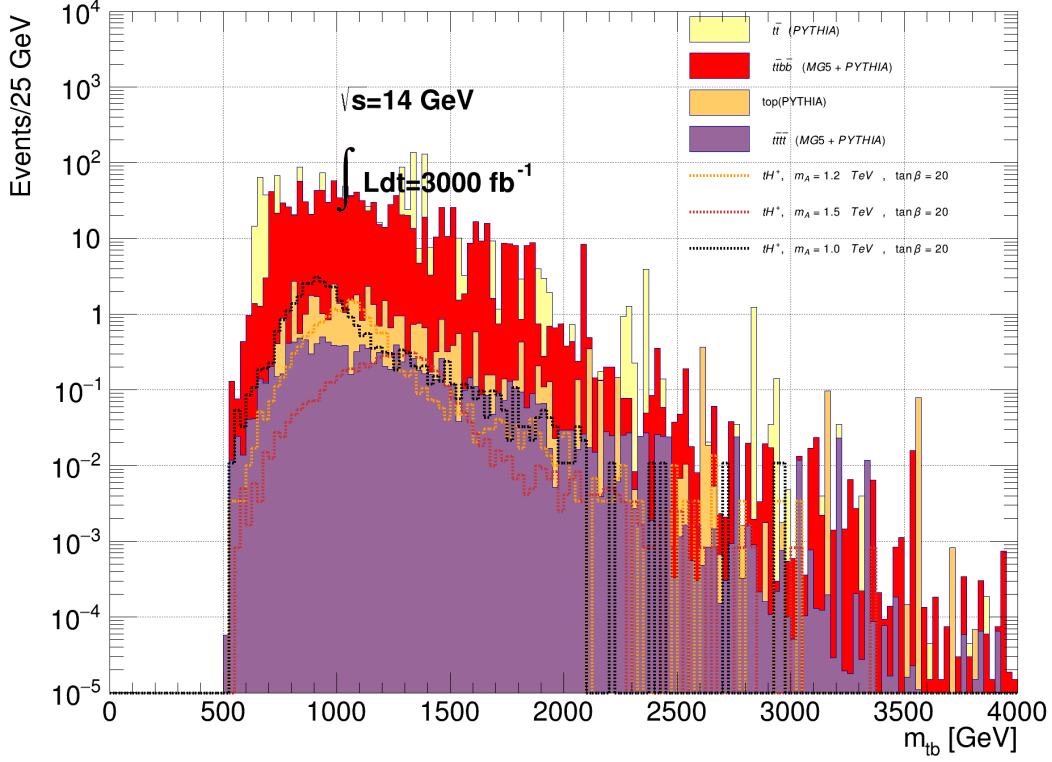


Figure 11: Distribution in  $m(tb)$  from  $pp \rightarrow H^\pm t + X$  followed by  $H^\pm \rightarrow tb$  decay. We also require that there is no fat jet tagged as a top-jet by HEPTopTagger2 but that there is an isolated lepton from the decay of one of the top quarks. We also show dominant SM backgrounds.

out to  $m_A \sim 1.6$  TeV for  $\tan \beta \sim 50$ . The discovery region pinches off below  $\tan \beta \sim 25$  where the signal, after analysis cuts, becomes too small relative to the standard model background. Unfortunately, the entire discovery region lies within the portion of the plane that already appears to be excluded by the ATLAS search for  $H/A \rightarrow \tau\tau$  decays [46].

In frame *b*), we plot the 95% CL exclusion limit for HL-LHC for our combined four signal channels. The exclusion limit now extends out to  $m_A \sim 2.1$  TeV for large  $\tan \beta \sim 50$ , and well outside the ATLAS excluded region denoted by the dashed blue line. We also see that the exclusion contour extends somewhat below  $\tan \beta \sim 20$  for lighter  $m_{H^+} \sim 1$  TeV. Also, a small exclusion region has now appeared at low  $\tan \beta \sim 3$ , which has also appeared in the ATLAS analysis [35].

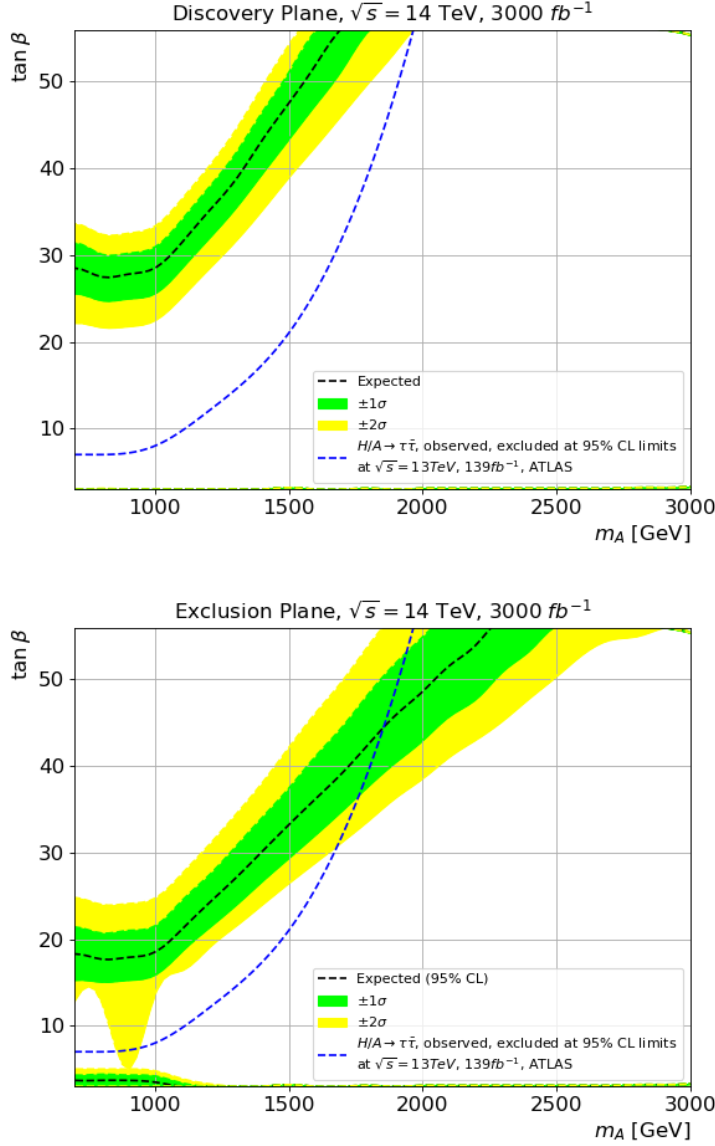


Figure 12: In *a*), we plot the  $5\sigma$  discovery region of the  $m_A$  vs.  $\tan\beta$  plane for  $pp \rightarrow H^\pm t + X$  followed by  $H^\pm \rightarrow tb$  decay for HL-LHC with  $3000 \text{ fb}^{-1}$ . In *b*), we plot the corresponding 95% CL exclusion region. The dashed blue line shows the boundary of the region excluded at the 95% confidence level in Ref. [46].

## 7 Search for $H^\pm \rightarrow \text{SUSY}$ at HL-LHC

In Ref. [3], we examined  $s$ -channel production of heavy neutral SUSY Higgs bosons followed by decays to SUSY particles, where in natural SUSY  $H, A \rightarrow \text{gaugino} + \text{higgsino}$  was the dominant decay mode (when kinematically open) except where  $\tan\beta$  was very large. The heavier higgsinos decay to soft visible particles plus  $\cancel{E}_T$  whilst the gauginos decay via  $W, Z, h + \cancel{E}_T$ . This led



to discovery channels of  $H$ ,  $A \rightarrow W$ ,  $Z$ ,  $h + \cancel{E}_T$  at HL-LHC, with accessible parameter regions mapped out in the  $m_A$  vs.  $\tan\beta$  plane for natSUSY in Ref. [3]. The number of signal events after cuts were typically in the range of tens of events at best at HL-LHC with  $3000 \text{ fb}^{-1}$  of integrated luminosity.

The question here is then: are there lucrative *charged* Higgs  $H^\pm \rightarrow \text{SUSY}$  decay channels available for HL-LHC? We saw in Fig. 3 that for moderate  $\tan\beta$  and  $m_{H^\pm} > m(\text{gaugino}) + m(\text{higgsino})$  that the SUSY decay modes also become the dominant decay channels for charged Higgs bosons. And like their neutral Higgs counterparts, the final state configurations for  $H^\pm \rightarrow \text{SUSY}$  end up being  $H^\pm \rightarrow W$ ,  $Z$ ,  $h + \cancel{E}_T$  according to the various charged Higgs and sparticle branching fractions from Isajet [39].

Thus, we have also examined the prospects for  $pp \rightarrow tH^\pm \rightarrow t + \text{SUSY} \rightarrow t + (W, Z, h) + \cancel{E}_T$  at HL-LHC. An essential difference of  $pp \rightarrow tH^\pm + X$  compared to  $pp \rightarrow H, A + X$  at LHC is that for a given heavy Higgs mass, the top-quark plus charged Higgs cross section is typically suppressed by an order of magnitude or more from  $s$ -channel neutral heavy Higgs production. A plot of charged Higgs production cross section times  $BF(H^\pm \rightarrow \text{SUSY})$  in fb in the  $m_A$  vs.  $\tan\beta$  plane is shown in Fig. 13 for the  $m_h^{125}(\text{nat})$  scenario. From the plot, for  $m_A \gtrsim 1 \text{ TeV}$  where decays to SUSY particles begin to become important, the cross sections lie in the sub-fb regime. In addition, one typically tries to tag the spectator  $t$ - or  $b$ -jet in  $tH^\pm$  production which also leads to a reduction in signal level. Then one must factor in further SUSY decay branching fractions to  $W$ ,  $Z$ ,  $h + \cancel{E}_T$  along with  $W$ ,  $Z$ ,  $h$  branching fractions into observable final states. The upshot is: the reduced signal channels compared to SM backgrounds  $t\bar{t}$ ,  $t\bar{t}b\bar{b}$ ,  $t\bar{t}W$ ,  $t\bar{t}Z$ ,  $t\bar{t}h$  etc. did not lead to any compelling discovery channels that we could find.

## 8 Regions of the $m_A$ vs. $\tan\beta$ plane accessible to HL-LHC via charged and neutral Higgs boson searches in natSUSY

We have found so far that a charged Higgs boson signal should be accessible to the HL-LHC in two different channels:  $H^\pm \rightarrow \tau\nu_\tau$  and, to a lesser degree, via  $H^\pm \rightarrow tb$ . The regions of the  $m_A$  vs.  $\tan\beta$  plane which are available to HL-LHC via  $5\sigma$  discovery and 95% CL exclusion have been mapped out. At this point, it is worthwhile to compare the reach of HL-LHC via charged Higgs boson searches to the reach which can be achieved via  $s$ -channel  $H$  and  $A$  signals as delineated for natSUSY in Ref. [2] and [3].

In Fig. 14, we plot out the  $5\sigma$  reach of HL-LHC with  $3000 \text{ fb}^{-1}$  in the  $m_A$  vs.  $\tan\beta$  plane for heavy charged and neutral Higgs boson signals in the natSUSY scenario. The red dashed contour shows the computed  $5\sigma$  discovery reach via the  $H$ ,  $A \rightarrow \tau\bar{\tau}$  channel. Of all channels assessed so far, this provides the maximal discovery reach due to higher production cross sections  $pp \rightarrow H, A + X$ , lower backgrounds in the ditau decay channel and the capability to reconstruct the ditau invariant mass  $m(\tau\bar{\tau})$  using the ability to roughly reconstruct the missing neutrino momentum. The discovery region lies above the contour which extends from  $\tan\beta \sim 8$  for  $m_A = 1 \text{ TeV}$  to  $\tan\beta \sim 35$  for  $m_A = 2.4 \text{ TeV}$ . The decay branching fraction for  $A \rightarrow \tau\bar{\tau}$  is of course enhanced by the well-known factor  $\tan^2\beta$ .

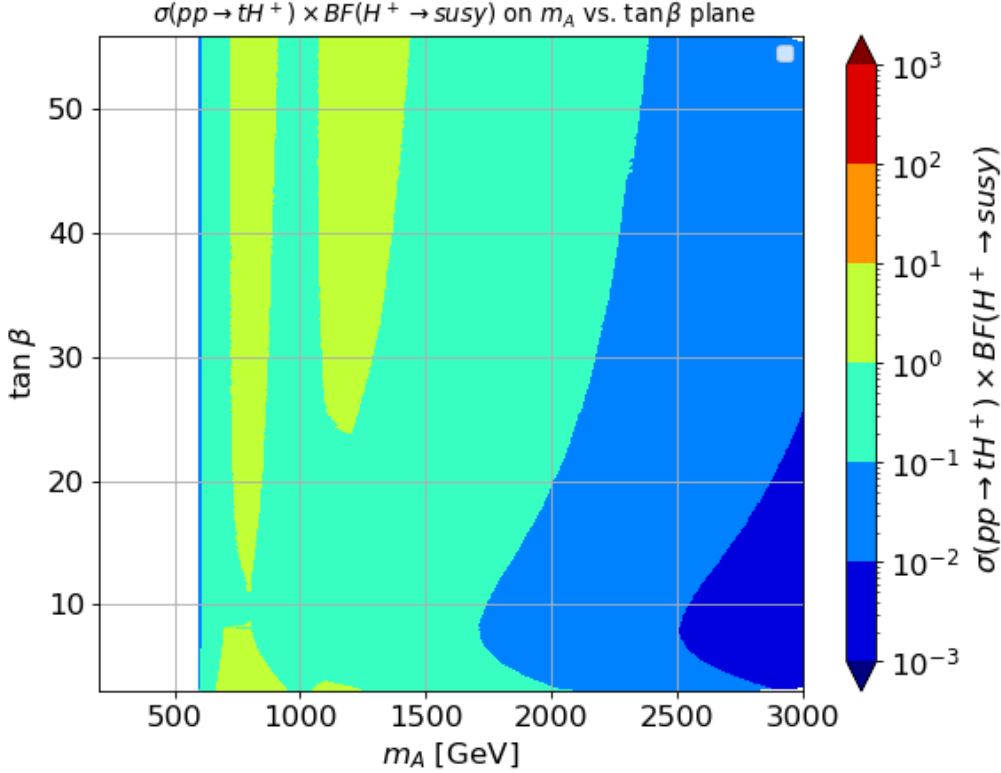


Figure 13: Plot of charged Higgs production cross section times  $BF(H^\pm \rightarrow SUSY)$  in fb in the  $m_A$  vs.  $\tan\beta$  plane for the  $m_h^{125}(\text{nat})$  scenario.

Next most important is the yellow-dashed contour for  $pp \rightarrow H, A$  with  $H, A \rightarrow SUSY \rightarrow (W, Z, h) + \cancel{E}_T$ . These combined channels determine the ultimate reach and only turn on for  $m_A \gtrsim 1$  TeV where  $H, A \rightarrow SUSY$  becomes kinematically accessible in the natSUSY scenario. The reach via SUSY decays is comparable with the  $H, A \rightarrow \tau\bar{\tau}$  reach for  $m_A \sim 1.2$  TeV, but for  $m_A \gtrsim 1.5$  TeV, the reach via SUSY decays drops off more quickly for larger  $\tan\beta$  values mainly because the  $H$  and  $A$  decays to SM fermions are enhanced by large Yukawa couplings, suppressing the branching fractions for decays to SUSY particles. The green-dashed contour denotes the HL-LHC  $5\sigma$  discovery reach via  $pp \rightarrow tH^\pm + X$  followed by  $H^\pm \rightarrow \tau\nu_\tau$  decay. For a given  $m_A$ , the  $pp \rightarrow tH^\pm + X$  cross section is well below the resonantly enhanced  $pp \rightarrow H, A$  and furthermore one cannot reconstruct a charged Higgs invariant mass via the  $H^\pm \rightarrow \tau\nu$  channel: as a result, the reach via the charged Higgs channel is substantially less than the the reach via  $pp \rightarrow H, A \rightarrow \tau\bar{\tau}$ . The blue dashed contour denotes the  $5\sigma$  discovery reach for  $pp \rightarrow tH^\pm + X$  with  $H^\pm \rightarrow tb$ . This discovery region is mainly applicable at large  $\tan\beta$ . Within the model, a substantial region of parameter space is accessible to HL-LHC via several discovery channels, but we should keep in mind that portions of this plane is excluded by the ATLAS search, albeit in a model with decoupled superpartners [46].

In Fig. 15, we show all four contours, but now as 95% CL exclusion limits, should no

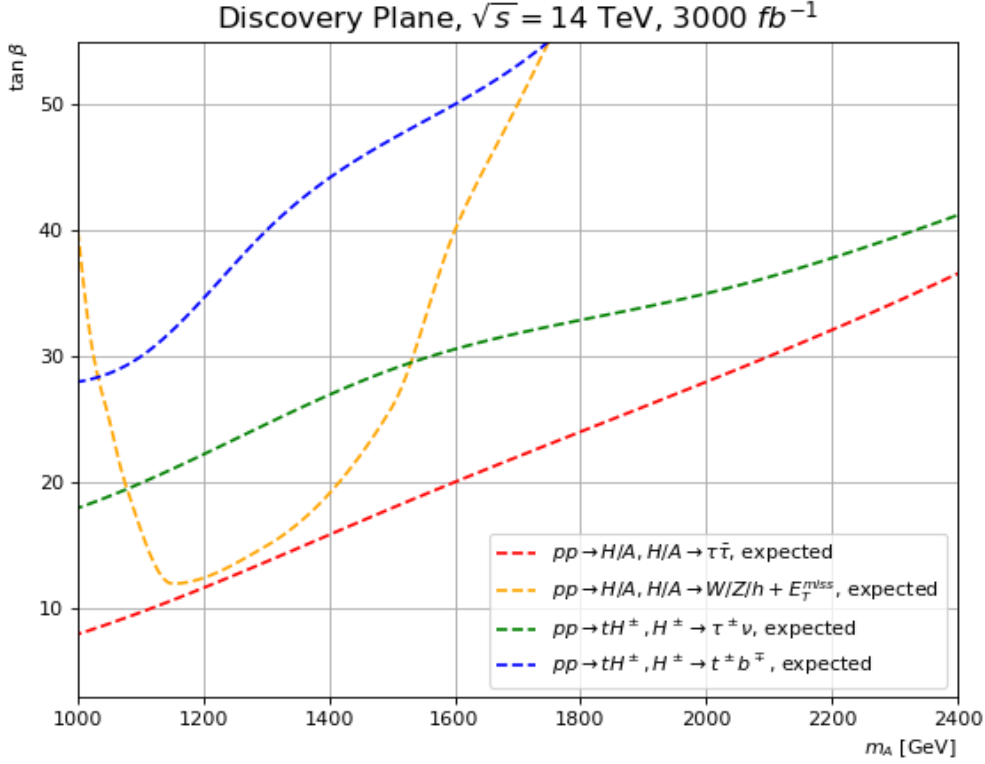


Figure 14: Plot of  $5\sigma$  discovery projections for heavy SUSY Higgs boson searches at HL-LHC in the  $m_A$  vs.  $\tan\beta$  plane for the  $m_h^{125}(\text{nat})$  scenario.

signal appear at the HL-LHC. For  $m_A \gtrsim 1.6$  TeV, the main exclusion would come from not discovering  $H, A \rightarrow \tau\bar{\tau}$  while for lower  $m_A \lesssim 1.6$  TeV the main exclusion come from not discovering  $H, A \rightarrow \text{SUSY} \rightarrow (W, Z, h) + \cancel{E}_T$ , where the exclusion contour dips to very low  $\tan\beta \sim 3$  (where  $m_h$  becomes lighter than 125 GeV). The charged Higgs exclusion contours are contained within the  $H, A \rightarrow \tau\bar{\tau}$  exclusion contour.

## 9 Conclusions

In this paper we have investigated the ability of HL-LHC to discover the charged Higgs bosons of supersymmetric theories in the natural SUSY scenario. We believe that the natSUSY scenario is strongly motivated in that it naturally explains the measured magnitude of the weak scale which arises from a conspiracy of the weak scale soft terms:  $\mu \sim 100 - 400$  GeV while  $m_{H_u}^2$  is radiatively driven to rather small negative values at the weak scale (EW symmetry is barely broken). Other sparticle masses can be much larger, lying in the TeV or beyond region since their contributions to the weak scale are suppressed (at least) by loop factors. Unnatural SUSY models which predict much higher values for  $m_{\text{weak}}$  are regarded as rather implausible since

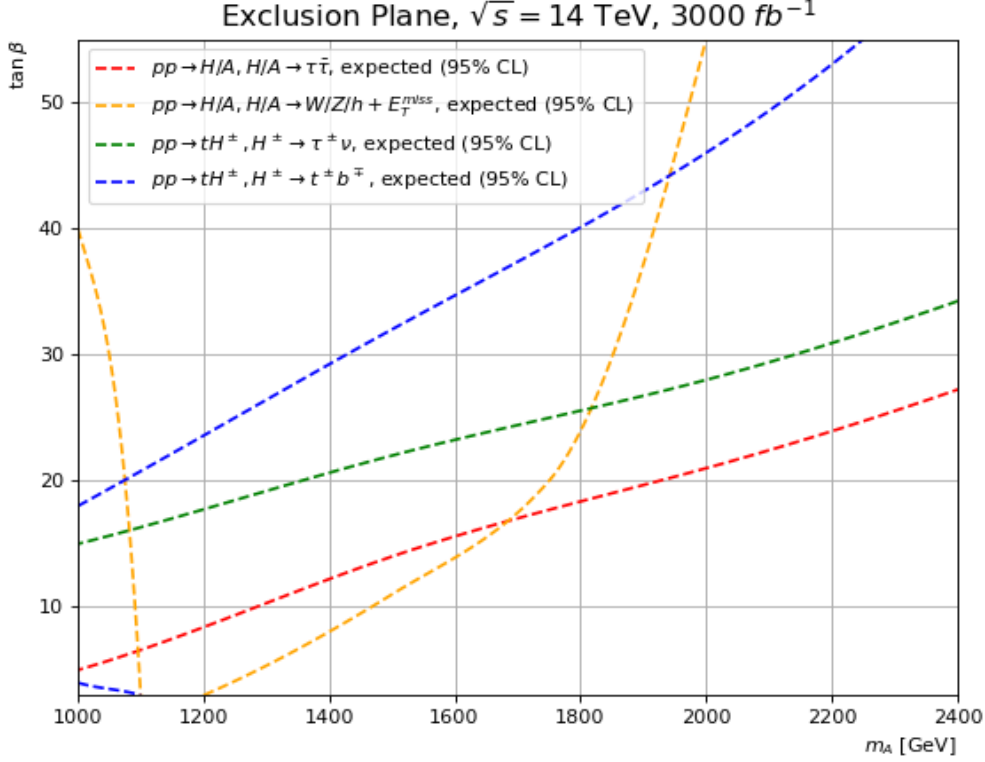


Figure 15: Plot of 95% CL exclusion projections for heavy SUSY Higgs boson searches at HL-LHC in the  $m_A$  vs.  $\tan \beta$  plane for the  $m_h^{125}(\text{nat})$  scenario.

they will require an unnatural conspiracy/finetuning of parameters in order to gain  $m_{\text{weak}} \sim 100$  GeV.

The charged Higgs boson masses can range from their present lower limits from LHC searches up into the multi-TeV range (depending on  $\tan \beta$ ) with little cost to EW naturalness. Furthermore, once their masses exceed  $m(\text{higgsino}) + m(\text{gaugino})$ , then the decay to SUSY particles can become dominant. This reduces heavy Higgs decay to SM particle signals as expected in unnatural scenarios such as 2HDMs, but also opens up possible new avenues for heavy Higgs discovery. In this paper, we have delineated search strategies for charged Higgs bosons in both the  $H^\pm \rightarrow \tau \nu_\tau$  and  $H^\pm \rightarrow tb$  channels and have also computed the regions of  $m_A$  vs.  $\tan \beta$  parameter space which are accessible to HL-LHC as the  $5\sigma$  and 95% CL contours. The HL-LHC reach for charged Higgs bosons is typically contained within the stronger reach via  $s$ -channel production of heavy neutrals  $H$  and  $A$ . For searches at the HL-LHC, decays of the charged Higgs boson to superpartners appear to be unimportant. Nonetheless, there do exist regions where all of  $H^\pm$ ,  $H$  and  $A$  may be discovered.

*Acknowledgements:*

This material is based upon work supported by the U.S. Department of Energy, Office of Science, Office of High Energy Physics under Award Number DE-SC-0009956 and DE-SC-

## References

- [1] H. Baer, X. Tata, Weak scale supersymmetry: From superfields to scattering events, Cambridge University Press, 2006.
- [2] H. Baer, V. Barger, X. Tata, K. Zhang, Prospects for Heavy Neutral SUSY HIGGS Scalars in the hMSSM and Natural SUSY at LHC Upgrades, *Symmetry* 14 (10) (2022) 2061. [arXiv:2209.00063](#), [doi:10.3390/sym14102061](#).
- [3] H. Baer, V. Barger, X. Tata, K. Zhang, Detecting Heavy Neutral SUSY Higgs Bosons Decaying to Sparticles at the High-Luminosity LHC, *Symmetry* 15 (2) (2023) 548. [arXiv:2212.09198](#), [doi:10.3390/sym15020548](#).
- [4] H. Baer, V. Barger, P. Huang, D. Mickelson, A. Mustafayev, X. Tata, Radiative natural supersymmetry: Reconciling electroweak fine-tuning and the Higgs boson mass, *Phys. Rev. D* 87 (11) (2013) 115028. [arXiv:1212.2655](#), [doi:10.1103/PhysRevD.87.115028](#).
- [5] H. Baer, V. Barger, D. Martinez, Comparison of SUSY spectra generators for natural SUSY and string landscape predictions, *Eur. Phys. J. C* 82 (2) (2022) 172. [arXiv:2111.03096](#), [doi:10.1140/epjc/s10052-022-10141-2](#).
- [6] A. Dedes, P. Slavich, Two loop corrections to radiative electroweak symmetry breaking in the MSSM, *Nucl. Phys. B* 657 (2003) 333–354. [arXiv:hep-ph/0212132](#), [doi:10.1016/S0550-3213\(03\)00173-1](#).
- [7] H. Baer, V. Barger, M. Savoy, Upper bounds on sparticle masses from naturalness or how to disprove weak scale supersymmetry, *Phys. Rev. D* 93 (3) (2016) 035016. [arXiv:1509.02929](#), [doi:10.1103/PhysRevD.93.035016](#).
- [8] H. Baer, V. Barger, D. Martinez, S. Salam, On practical naturalness and its implications for weak scale supersymmetry (5 2023). [arXiv:2305.16125](#).
- [9] H. Baer, V. Barger, P. Huang, A. Mustafayev, X. Tata, Radiative natural SUSY with a 125 GeV Higgs boson, *Phys. Rev. Lett.* 109 (2012) 161802. [arXiv:1207.3343](#), [doi:10.1103/PhysRevLett.109.161802](#).
- [10] K. J. Bae, H. Baer, V. Barger, D. Sengupta, Revisiting the SUSY  $\mu$  problem and its solutions in the LHC era, *Phys. Rev. D* 99 (11) (2019) 115027. [arXiv:1902.10748](#), [doi:10.1103/PhysRevD.99.115027](#).
- [11] H. Baer, V. Barger, D. Martinez, S. Salam, Fine-tuned vs. natural supersymmetry: what does the string landscape predict? (6 2022). [arXiv:2206.14839](#).
- [12] K. J. Bae, H. Baer, V. Barger, D. Mickelson, M. Savoy, Implications of naturalness for the heavy Higgs bosons of supersymmetry, *Phys. Rev. D* 90 (7) (2014) 075010. [arXiv:1407.3853](#), [doi:10.1103/PhysRevD.90.075010](#).

- [13] A. C. Bawa, C. S. Kim, A. D. Martin, Charged Higgs Production at Hadron Colliders, *Z. Phys. C* 47 (1990) 75–82. doi:10.1007/BF01551915.
- [14] J. F. Gunion, Detecting the  $t\bar{b}$  decays of a charged Higgs boson at a hadron supercollider, *Phys. Lett. B* 322 (1994) 125–130. arXiv:hep-ph/9312201, doi:10.1016/0370-2693(94)90500-2.
- [15] V. D. Barger, R. J. N. Phillips, D. P. Roy, Heavy charged Higgs signals at the LHC, *Phys. Lett. B* 324 (1994) 236–240. arXiv:hep-ph/9311372, doi:10.1016/0370-2693(94)90413-8.
- [16] H. Baer, X. Tata, Implications of the  $t$  Quark Signal for Stop Squarks and Charged Higgs Bosons, *Phys. Lett. B* 167 (1986) 241–247. doi:10.1016/0370-2693(86)90607-6.
- [17] Z. Kunszt, F. Zwirner, Testing the Higgs sector of the minimal supersymmetric standard model at large hadron colliders, *Nucl. Phys. B* 385 (1992) 3–75. arXiv:hep-ph/9203223, doi:10.1016/0550-3213(92)90094-R.
- [18] H. Baer, D. Dicus, M. Drees, X. Tata, Higgs Boson Signals in Superstring Inspired Models at Hadron Supercolliders, *Phys. Rev. D* 36 (1987) 1363. doi:10.1103/PhysRevD.36.1363.
- [19] J. F. Gunion, H. E. Haber, M. Drees, D. Karatas, X. Tata, R. Godbole, N. Tracas, Decays of Higgs Bosons to Neutralinos and Charginos in the Minimal Supersymmetric Model: Calculation and Phenomenology, *Int. J. Mod. Phys. A* 2 (1987) 1035. doi:10.1142/S0217751X87000442.
- [20] J. F. Gunion, H. E. Haber, Higgs Bosons in Supersymmetric Models. 3. Decays Into Neutralinos and Charginos, *Nucl. Phys. B* 307 (1988) 445, [Erratum: *Nucl.Phys.B* 402, 569 (1993)]. doi:10.1016/0550-3213(88)90259-3.
- [21] H. Baer, M. Bisset, D. Dicus, C. Kao, X. Tata, The Search for Higgs bosons of minimal supersymmetry: Impact of supersymmetric decay modes, *Phys. Rev. D* 47 (1993) 1062–1079. doi:10.1103/PhysRevD.47.1062.
- [22] T. Plehn, Charged Higgs boson production in bottom gluon fusion, *Phys. Rev. D* 67 (2003) 014018. arXiv:hep-ph/0206121, doi:10.1103/PhysRevD.67.014018.
- [23] E. L. Berger, T. Han, J. Jiang, T. Plehn, Associated production of a top quark and a charged Higgs boson, *Phys. Rev. D* 71 (2005) 115012. arXiv:hep-ph/0312286, doi:10.1103/PhysRevD.71.115012.
- [24] S.-h. Zhu, Complete next-to-leading order QCD corrections to charged Higgs boson associated production with top quark at the CERN large hadron collider, *Phys. Rev. D* 67 (2003) 075006. arXiv:hep-ph/0112109, doi:10.1103/PhysRevD.67.075006.
- [25] D. P. Roy, The Hadronic  $\tau$  decay signature of a heavy charged Higgs boson at LHC, *Phys. Lett. B* 459 (1999) 607–614. arXiv:hep-ph/9905542, doi:10.1016/S0370-2693(99)00724-8.

- [26] K. A. Assamagan, Y. Coadou, The hadronic tau decay of a heavy  $H^{\pm}$  in ATLAS, *Acta Phys. Polon. B* 33 (2002) 707–720.
- [27] M. Drees, M. Guchait, D. P. Roy, Signature of charged to neutral Higgs boson decay at the LHC in SUSY models, *Phys. Lett. B* 471 (1999) 39–44. [arXiv:hep-ph/9909266](#), [doi:10.1016/S0370-2693\(99\)01329-5](#).
- [28] S. Moretti, D. P. Roy, Detecting heavy charged Higgs bosons at the LHC with triple  $b$  tagging, *Phys. Lett. B* 470 (1999) 209–214. [arXiv:hep-ph/9909435](#), [doi:10.1016/S0370-2693\(99\)01291-5](#).
- [29] D. J. Miller, S. Moretti, D. P. Roy, W. J. Stirling, Detecting heavy charged Higgs bosons at the CERN LHC with four  $b$  quark tags, *Phys. Rev. D* 61 (2000) 055011. [arXiv:hep-ph/9906230](#), [doi:10.1103/PhysRevD.61.055011](#).
- [30] M. Carena, D. Garcia, U. Nierste, C. E. M. Wagner, Effective Lagrangian for the  $\bar{t}bH^+$  interaction in the MSSM and charged Higgs phenomenology, *Nucl. Phys. B* 577 (2000) 88–120. [arXiv:hep-ph/9912516](#), [doi:10.1016/S0550-3213\(00\)00146-2](#).
- [31] D. Denegri, V. Drollinger, R. Kinnunen, K. Lassila-Perini, S. Lehti, F. Moortgat, A. Nikitenko, S. Slabospitsky, N. Stepanov, Summary of the CMS discovery potential for the MSSM SUSY Higgses (11 2001). [arXiv:hep-ph/0112045](#).
- [32] K. A. Assamagan, Y. Coadou, A. Deandrea, ATLAS discovery potential for a heavy charged Higgs boson, *Eur. Phys. J. direct* 4 (1) (2002) 9. [arXiv:hep-ph/0203121](#), [doi:10.1007/s1010502c0009](#).
- [33] M. Aaboud, et al., Search for charged Higgs bosons decaying via  $H^{\pm} \rightarrow \tau^{\pm}\nu_{\tau}$  in the  $\tau$ +jets and  $\tau$ +lepton final states with  $36\text{ fb}^{-1}$  of  $pp$  collision data recorded at  $\sqrt{s} = 13$  TeV with the ATLAS experiment, *JHEP* 09 (2018) 139. [arXiv:1807.07915](#), [doi:10.1007/JHEP09\(2018\)139](#).
- [34] A. M. Sirunyan, et al., Search for charged Higgs bosons in the  $H^{\pm} \rightarrow \tau^{\pm}\nu_{\tau}$  decay channel in proton-proton collisions at  $\sqrt{s} = 13$  TeV, *JHEP* 07 (2019) 142. [arXiv:1903.04560](#), [doi:10.1007/JHEP07\(2019\)142](#).
- [35] G. Aad, et al., Search for charged Higgs bosons decaying into a top quark and a bottom quark at  $\sqrt{s} = 13$  TeV with the ATLAS detector, *JHEP* 06 (2021) 145. [arXiv:2102.10076](#), [doi:10.1007/JHEP06\(2021\)145](#).
- [36] A. Arhrib, R. Benbrik, H. Harouiz, S. Moretti, A. Rouchad, A Guidebook to Hunting Charged Higgs Bosons at the LHC, *Front. in Phys.* 8 (2020) 39. [arXiv:1810.09106](#), [doi:10.3389/fphy.2020.00039](#).
- [37] A. G. Akeroyd, et al., Prospects for charged Higgs searches at the LHC, *Eur. Phys. J. C* 77 (5) (2017) 276. [arXiv:1607.01320](#), [doi:10.1140/epjc/s10052-017-4829-2](#).

- [38] H. Baer, A. Mustafayev, S. Profumo, A. Belyaev, X. Tata, Direct, indirect and collider detection of neutralino dark matter in SUSY models with non-universal Higgs masses, JHEP 07 (2005) 065. [arXiv:hep-ph/0504001](#), [doi:10.1088/1126-6708/2005/07/065](#).
- [39] F. E. Paige, S. D. Protopopescu, H. Baer, X. Tata, ISAJET 7.69: A Monte Carlo event generator for pp, anti-p p, and e+e- reactions (12 2003). [arXiv:hep-ph/0312045](#).
- [40] H. Baer, C.-H. Chen, R. B. Munroe, F. E. Paige, X. Tata, Multichannel search for minimal supergravity at  $p\bar{p}$  and  $e^+e^-$  colliders, Phys. Rev. D 51 (1995) 1046–1050. [arXiv:hep-ph/9408265](#), [doi:10.1103/PhysRevD.51.1046](#).
- [41] M. A. Bisset, Detection of Higgs bosons of the minimal supersymmetric standard model at hadron supercolliders, University of hawaii doctoral thesis umi-95-32579 (May, 1995).
- [42] D. M. Pierce, J. A. Bagger, K. T. Matchev, R.-j. Zhang, Precision corrections in the minimal supersymmetric standard model, Nucl. Phys. B 491 (1997) 3–67. [arXiv:hep-ph/9606211](#), [doi:10.1016/S0550-3213\(96\)00683-9](#).
- [43] M. Carena, H. E. Haber, Higgs Boson Theory and Phenomenology, Prog. Part. Nucl. Phys. 50 (2003) 63–152. [arXiv:hep-ph/0208209](#), [doi:10.1016/S0146-6410\(02\)00177-1](#).
- [44] T. Sjostrand, S. Mrenna, P. Z. Skands, A Brief Introduction to PYTHIA 8.1, Comput. Phys. Commun. 178 (2008) 852–867. [arXiv:0710.3820](#), [doi:10.1016/j.cpc.2008.01.036](#).
- [45] D. A. Dicus, J. L. Hewett, C. Kao, T. G. Rizzo,  $W^+H^-$  Production at Hadron Collider, Phys. Rev. D 40 (1989) 787. [doi:10.1103/PhysRevD.40.787](#).
- [46] G. Aad, et al., Search for heavy Higgs bosons decaying into two tau leptons with the ATLAS detector using  $pp$  collisions at  $\sqrt{s} = 13$  TeV, Phys. Rev. Lett. 125 (5) (2020) 051801. [arXiv:2002.12223](#), [doi:10.1103/PhysRevLett.125.051801](#).
- [47] J. Alwall, M. Herquet, F. Maltoni, O. Mattelaer, T. Stelzer, MadGraph 5 : Going Beyond, JHEP 06 (2011) 128. [arXiv:1106.0522](#), [doi:10.1007/JHEP06\(2011\)128](#).
- [48] J. de Favereau, C. Delaere, P. Demin, A. Giammanco, V. Lemaître, A. Mertens, M. Selvaggi, DELPHES 3, A modular framework for fast simulation of a generic collider experiment, JHEP 02 (2014) 057. [arXiv:1307.6346](#), [doi:10.1007/JHEP02\(2014\)057](#).
- [49] A. L. Read, Presentation of search results: the  $CL_s$  technique, J. Phys. G 28 (2002) 2693. [doi:10.1088/0954-3899/28/10/313](#).
- [50] G. Cowan, K. Cranmer, E. Gross, O. Vitells, Asymptotic formulae for likelihood-based tests of new physics, Eur.Phys. J. C 71 (2011). [arXiv:1007.1727](#), [doi:10.1140/epjc/s10052-011-1554-0](#).
- [51] H. Baer, V. Barger, S. Salam, D. Sengupta, K. Sinha, Status of weak scale supersymmetry after LHC Run 2 and ton-scale noble liquid WIMP searches, Eur. Phys. J. ST 229 (21) (2020) 3085–3141. [arXiv:2002.03013](#), [doi:10.1140/epjst/e2020-000020-x](#).



- [52] A Cambridge-Aachen (C-A) based Jet Algorithm for boosted top-jet tagging, CMS-PAS-JME-09-001 (July, 2009).
- [53] C. Anders, C. Bernaciak, G. Kasieczka, T. Plehn, T. Schell, Benchmarking an even better top tagger algorithm, Phys. Rev. D 89 (7) (2014) 074047. [arXiv:1312.1504](#), [doi:10.1103/PhysRevD.89.074047](#).
- [54] T. Plehn, M. Spannowsky, M. Takeuchi, How to Improve Top Tagging, Phys. Rev. D 85 (2012) 034029. [arXiv:1111.5034](#), [doi:10.1103/PhysRevD.85.034029](#).
- [55] M. Aaboud, et al., Search for charged Higgs bosons decaying into top and bottom quarks at  $\sqrt{s} = 13$  TeV with the ATLAS detector, JHEP 11 (2018) 085. [arXiv:1808.03599](#), [doi:10.1007/JHEP11\(2018\)085](#).
- [56] D. Krohn, J. Thaler, L.-T. Wang, Jet Trimming, JHEP 02 (2010) 084. [arXiv:0912.1342](#), [doi:10.1007/JHEP02\(2010\)084](#).